Nano-MoS2 and Graphene Additives in Oil for Tribological Applications

Xu, Yufu; Peng, Yubin; You, Tao; Yao, Lulu; Geng, Jian; Dearn, Karl; Hu, Xianguo

DOI:
10.1007/978-3-319-60630-9_6

Nano-MoS_2 and Graphene Additives in Oil for Tribological Applications

Yufu Xu[a]*, Yubin Peng[a], Tao You[a], Lulu Yao[b], Jian Geng[a], Karl D. Dearn[c], Xianguo Hu[a]

a. *Institute of Tribology, School of Mechanical Engineering, Hefei University of Technology, Hefei 230009, China*

b. *School of Chemistry and Chemical Engineering, Hefei University of Technology, Hefei 230009, China*

c. *Department of Mechanical Engineering, School of Engineering, University of Birmingham, Edgbaston, Birmingham B152TT, United Kingdom*

Abstract: Nano-additives have attracted lots of attentions in recent years due to their special performances. A traditional lubricating additive MoS_2 with nano-scale and a novel additive graphene were reviewed in this chapter. The synthesis methods, properties and tribological applications of these two kinds of nano-additives dispersed in media have been reported. Nano-MoS_2 has three main nanostructures including nano-ball particles, nano-sheets and nano-tubes. The wide accepted lubricating mechanisms for the MoS_2 nano-balls, nano-sheets and nano-tubes are nano-bearing effects, slippery roles and combined actions of rolling and sliding, respectively. Exfoliation and transfer seems to be the main pattern for MoS_2 nano-balls. For graphene, the adsorption and tribo-reaction account for its lubricating properties. A synergistic lubricating

* Corresponding author. Tel.: +86 551 62901359; fax: +86 551 62901359.

E-mail: xuyufu@hfut.edu.cn

effect for using graphene and MoS_2 together dispersed in oil was found. Graphene was proved to extend the retention of MoS_2 on the surfaces and prevent the oxidation of MoS_2. Simultaneously, MoS_2 prevented the graphene from being ground into small and defective platelets. Both of them help to form a thicker adsorbed and tribo- film which result in a lower friction and wear. Other properties and applications of nano-MoS_2 and graphene are also reviewed. It shows that these two nano-additives have diverse functions and great potential for industrial applications.

Keywords: Nano-MoS_2; Graphene; Nano-additives; Tribological application

1. Introduction

A general demand from Society for a more sustainable and environmentally friendly development has led to an increasing interest and a growing corpus of work on energy-saving and emission reduction technologies [1]. The internal combustion engine is one such technology that has seen huge improvements in fuel efficiency, reduced overall energy consumption and emissions, and a key aspect of this has been improvements to the lubrication system [2].

With the development of the nanotechnologies, the use of nano additives added to base oils have been shown to reduce friction and wear due to their excellent lubricating effects. Some common solid particle lubricants such as nano-MoS_2 and graphene have made the transition from concept to application and are showing great potential in industry. However, there still exists a gap between the scientists and

industrial engineers, relating to a general willingness to use the new formulated additives [3]. However, if emissions and fuel consumption targets are to be met, then nano additives, added to lubricant formulations will be a vital component for industry to deploy to meet these objectives.

In this chapter, the progress and particularly the tribological behaviors of some key nano additives dispersed in base oil are reviewed, and the trends in future developments of nano additives is discussed in order to accelerate their application.

2. An introduction to and the tribological behaviour of Nano-MoS_2

Molybdenum disulfide (MoS_2) has a layered two-dimensional structure. Its crystal structure contains 1T-MoS_2, 2H-MoS_2 and 3R-MoS_2. 1T-MoS_2, per unit cell, has an octahedral structure with S atoms and one Mo atom; 2H-MoS_2 has a Mo atom with hexagonal structure and two S-Mo-S covalent bonds; and 3R-MoS_2 has a Mo atom with hexagonal structure and three S-Mo-S covalent bonds. Their respective structures are shown in **Fig. 1**. Among these MoS_2 crystals, 1T and 3R-MoS_2 are metastable and 2H-MoS_2 is stable under normal conditions. But no matter which crystal, each S atom is surrounded by 3 Mo atoms, and each Mo atom is surrounded with six S atoms consisting of S-Mo-S covalent bonds [4], such that the atom ratio of Mo and S is 1:2.

The layered structure of MoS_2 has excellent tribological properties which are attributed to a combination of its low Van der Waals force between the molecule layers and strong covalent bond in molecule. When MoS_2 bears a shear stress, molecular

layers slide easily over one another. Th is is the reason that MoS_2 has been widely used as a solid lubricant and used as an additive of lubricating oils. It has been proved that the size of MoS_2 particles has a significant affect their performances and so in the following section, some typical nano structures of MoS_2 are reviewed.

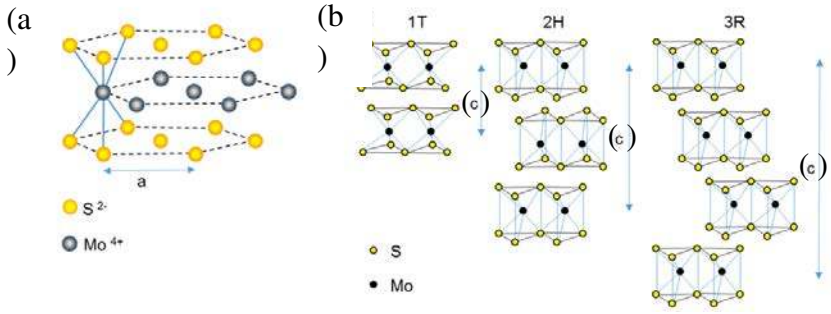

Figure 1. Hexagonal structure of MoS_2 (a), schematic illustration of the 1T- MoS_2 (b), 2H-MoS_2, and 3R-MoS_2, and the repeat unit of the MoS_2 layers (c) [5].

2.1 MoS_2 particles – nano-balls

Compared with MoS_2 sheets, MoS_2 nano-ball particles have some particular characteristics, including no dangling bonds that make them more stable. Additionally, the small size of the MoS_2 nano-particles may result in some other enhanced physical properties.

2.1.1 Preparation of MoS_2 nano-balls

Rosentsveig et al [6] used a four-step method to produce an inorganic fullerene-like (IF) MoS_2, which constitutes a typical nano-ball particle. The process includes four consecutive steps: (1) Evaporation of the molybdenum oxide (MoO_3) powder at a temperature of between 700–750 °C; (2) the reduction and condensation of the vapor

into MoO_{3-x} nanoparticles at 780 °C; (3) the sulfurization of the first few layers of the oxide nanoparticles; (4) The complete sulfurization of the nanoparticles with a slow diffusion-controlled reaction at a temperature above 840 °C. This method allows the sulfurized degree to be controlled (**Fig. 2**), it is however a complex procedure that consumes a large amount of energy.

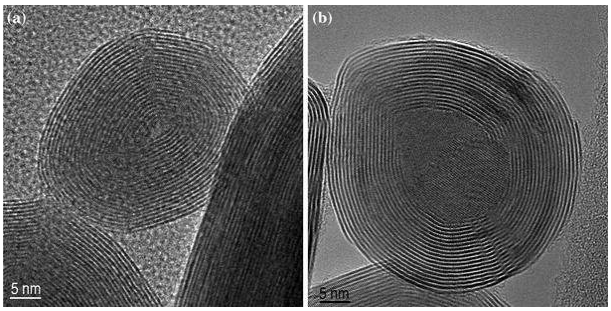

Figure 2. TEM images of IF-MoS_2 nanoparticles with no oxide (a), and remaining oxide (MoO_2) in the core (b) [6].

Precipitation is another popular approach used for producing MoS_2 nano-balls due to the relatively gentle synthesis conditions. As an example, Huang et al [7] added 28 g Na_2S and 5 g $(NH_4)_2MoO_4$ into 250 mL distilled water, allowing the reaction to occur over an hour. During the reaction, hydrochloric acid was added into the solution in order to control the acidic pH. After this, the as-prepared MoS_3 precursor was despulphurized in a gas mixture of hydrogen-argon at 1173 K for 8 h. The final nano-balls had diameters varying from 70 to 120 nm (Seen from **Fig. 3**).

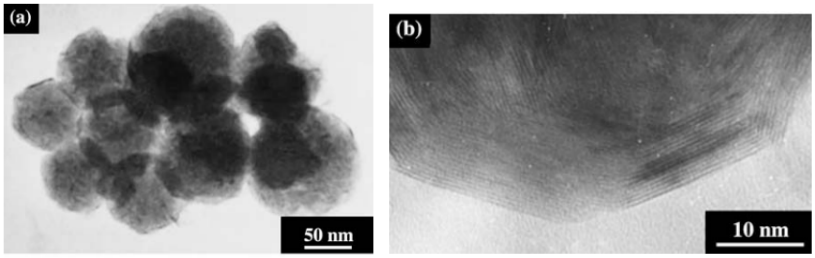

Figure 3. TEM images of the IF–MoS_2 nanoparticles from produced using precipitation methods [7].

Hu et al [8] prepared molybdenum sulphide particles with Na_2MoO_4 and CH_3CSNH_2 by a quick (c. 5 mins) homogenous precipitation technique in an alcohol–water solution at 82 °C. The resultant amorphous MoS_x nano-ball particles were then despulphurized under H_2 flow at an elevated temperature for 50 min. This method seems to be another alternative method that can be used to synthesize nano- ball MoS_2.

2.1.2 Characterization of MoS_2 nanoballs

Transmission electron microscopy (TEM) can be used to observe MoS_2 nano-particles, operating a levels of resolution that are much higher than light microscopes, due in part to the small de Broglie wavelength of electrons. It can also be used to show structure, morphology and to check the aggregation of nano-particles.

Scanning electron microscopy (SEM) is another effective tool to observe the form of nano-particles. As an example, **Fig. 4** [7], shows a MoS_3 precursor produced by Huang, with a clear spherical shape, with a diameter of ~150 nm. However, the aggregation of the nano-particles is severe as no dispersing media can be used with this method.

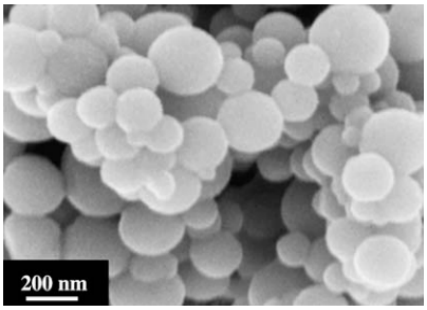

Figure 4. SEM image of MoS_3 precursor [7].

X-ray powder diffraction (XRD) can be used to assess the crystal structure of MoS_2 nano-particles. The work of the Institute of Tribology at Hefei University of Technology has proved that the MoS_2 nano particles have the similar XRD spectra in **Fig. 5** with the standard curve of MoS_2 in PDF number 37-1492. Its holly structures are also shown in TEM in **Fig. 5**.

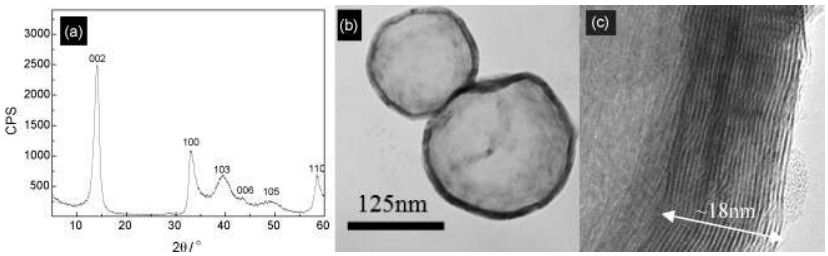

Figure 5. XRD (a), TEM (b) and HRTEM (c) of the MoS_2 nano-ball particles [9].

The crystallinity and shape of MoS_2 nano-balls are the main characteristics that affect frictional properties. These two properties are governed by the parameers and conditions slected during synthesis. Crystallinity governs the order degree of an MoS_2 layer which is composed of closed shells nano-balls. Perfectly crystalline MoS_2 nano-balls have a well crystalline order with few defects present in closed shells, whereas

poor crystallinity shows some extent of disorder with many point defects (**Fig. 6**). Moreover, perfectly crystalline MoS_2 nano-balls will have good physical properties. The shape of an MoS_2 nano-ball is not a perfect sphere most of the time. There are corners in the structure which are likely to induce stress concentrations. With this in mind, therefore the more perfectly crystalline and spherically shaped that the MoS_2 nano-ball is, the higher the ability resisting deformation [10].

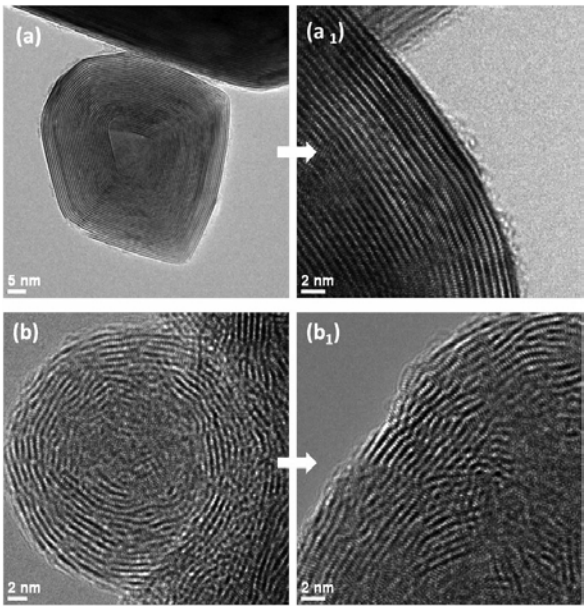

Figure 6. HRTEM images of perfect (a, a_1) and incomplete crystalline MoS_2 nano-balls (b, b_1) [10].

2.1.3 Dispersion of MoS_2 nano-balls in base oil

MoS_2 nano particles have lots of functions including lubrication, catalysis [11], functional materials and so on [12]. Among them, one of the most important function for MoS_2 seems to be lubrication. Usually, it is used as an additive in base oil or grease. Thus, the choice of the base oil is very important for improving the lubricating properties of MoS_2 nano-particles. For example, an industrial oil composed of many

fractions of hydrocarbons has been used for dispersing MoS_2 nanoparticles [13]. The industrial oil will have contained has many other additives with a variety of roles. To reduce the effects of the other additives, paraffin oil is often chosen as a base oil for use with MoS_2 nano-particles [7] because of the similar components with traditional mechanical oils. Poly alpha olefin (PAO) has attracted lots of attention, with excellent thermal stability and anti-oxidation properties, as base oil with MoS_2 nanoparticles in recent years [6]. Moreover, Xu et *al.* have tried some renewable bio-energies, such as bio-oil, as the base oil for MoS_2 micro-sheets, which have also shown good lubricating effects.

It has been reported that the addition of the nano-particles on their own in base oil has little effect on the tribological properties of a tribo-systems. But takes effects after using a dispersing agent [13-15]. This suggests that the selection of the dispersive agent and method of mixing are very important. Zhou et al [16] used an extractant Cyanex 301 (di-(2,4,4-trimethylpentyl) dithiophosphinic acid) to modify the surface of MoS_2 nano-hollow spheres in liquid paraffin. Results showed that the modified MoS_2 had better extreme pressure, antiwear and antifriction properties than commercial MoS_2. Sorbitol monooleate was selected by Huang et al. [7] as the dispersing agent for IF–MoS_2 in paraffin oil. The mixture was stirred with a high speed dispersion machine before ultrasonic treatment.

Dispersant agents can be grafted or adsorbed on nanoparticles with ultrasonication or stirring. The chemical affinity between dispersants and nanoparticles is main factor affect the dispersion. When chemical affinity is low, the particles can be easily

separated from the base oil and the nanoparticles will agglomerate again under the effect of friction [13].

It is important not to increase the concentration of dispersants to levels that are too high in the lubricant. Under such conditions, though the nanoparticles will be well dispersed, a large amount of dispersant agent, will reduce the life of the lubricant and increase friction. As shown in **Fig. 7**, the tribological benefits of MoS_2 were eliminated when 5% dispersant was used. However, when the dispersant concentration was adjusted to 0.05%, the friction coefficient decreased. The reason for this is that with high concentraions of dispersants, MoS_2 nanoparticles, MoS_2 cannot be adsorbed on the rubbing surface and reduced the friction coefficient [17].

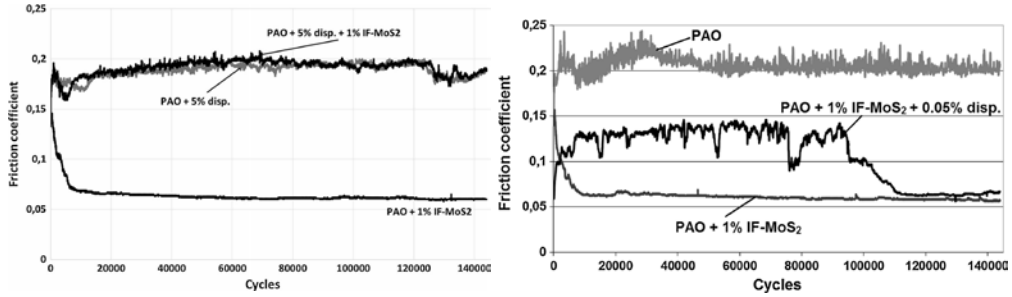

Figure 7. Friction coefficient of PAO +1% IF-MoS_2+5% dispersant (left),and PAO +1% IF-MoS_2+0.05% dispersant (right) [17].

2.1.4 Comparison with micro-MoS_2

MoS_2 nano particles have better lubricating properties than MoS_2 micro particles [18]. According to the Risdon's investigation [19], the energy consumed on transportation in the US during the period 1963-1974 can be reduced by 4.4% with proper dispersion of 1% weight commercial molybdenum disulfide in the engine oil. Thus, it

can be inferred that more fuel can be saved by the introduction of nano-MoS_2. Hu's results [18] showed that the addition of MoS_2 nano-balls in liquid paraffin at a concentration of 1.5 wt% resulted in a better antifriction and antiwear properties than micro-MoS_2. **Fig. 8** shows a friction coefficient reducedion of 21% and 10% respectively, when compared to those of 1.5% micro-MoS_2 and 1.0% nano-slices.

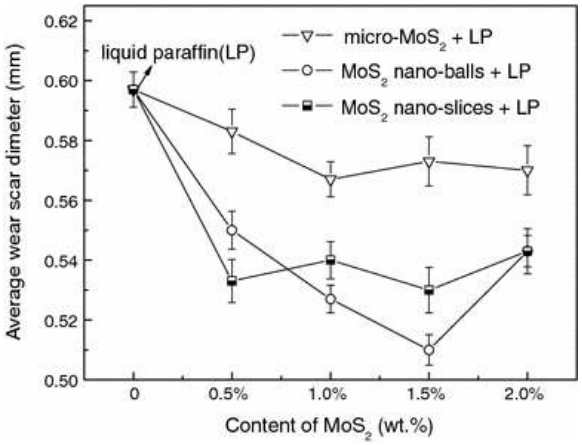

Figure 8. Effects of the concentration of MoS_2 on the average wear scar [18].

2.1.5 Effect of ZDDP on tribological properties

ZDDP (Zinc Dialkyl Dithiophosphates) is an important oxidation and corrosion inhibitor often found in full formulated lubricating oil which extends the oxidation resistance of lubricating oil. It also has excellent anti-wear properties but has no effect on friction. Lamellar MoS_2 nanoparticles derived from nano-sheets or the exfoliation of nanoballs are easily oxidized to MoO_3 which degrade the friction-reducing properties of MoS_2. When ZDDP and MoS_2 nanoparticles exist together, both friction coefficient and wear are reduced significantly. It is believed that there is a synergistic effect between ZDDP and MoS_2: the MoS_2 is believed to be embedded into ZDDP chemical reaction film and therefore reinforces its anti-wear effect, at the same time,

the ZDDP film provides protection for the MoS_2 from being oxidized resulting in the improvement of the antifriction behaviors [20, 21].

2.1.6 Effect of crystallinity on tribological properties

The tribological properties of MoS_2 nanoballs to some extent are dependant on its structural characteristics and particularly its crystallinity. MoS_2 nanoballs that are perfectly crystalline have a better ability to resist deformation, whereas MoS_2 with incomplete crystallinity are easily deformed and exfoliated under the similar sliding conditions [10]. Rabaso et al. [22] compared the frictional properties of MoS_2 with prefect and poorly crystalline structures with similar average diameters (150nm). They found that perfect MoS_2 nano-balls played a significant role in friction-reduction during running in, however, the friction coefficient increased after this due to the lack of perfect MoS_2 nano-balls. On the contrary, poorly crystalline MoS_2 maintained a stable low friction coefficient as shown in **Fig. 9**. The difference is because poorly crystalline can be easily exfoliated and transferred onto the rubbing surfaces forming an adsorbed layer. Perfect crystalline nano-particles were much harder to exfoliate before being squeezed out from the rubbing interfaces thanks to the better physical properties. In addition to the frictional process, the MoS_2 adsorbed film formed during the early stages of rubbing was gradually worn off. Due to the two reasons above, there were few MoS_2 particles remaining between the frictional interfaces resulting in the increase of the friction coefficient.

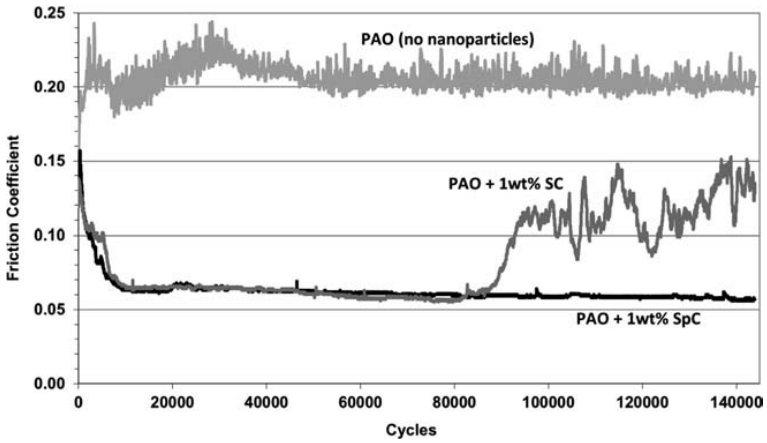

Figure 9. Friction coefficient of perfect (SC) and poorly crystalline (SpC) on HFRR [22].

2.1.7 Effect of different of pressure on exfoliation behavior

MoS_2 nano-balls can be ruptured under a high normal stress on the frictional interfaces. However, this will not happen in oil though oil pressure might be much higher than critical ruptured normal stress. That is because oil pressure is isotropic and the shape of the nano-ball is quasi-spherical which makes bearing force of MoS_2 uniform (**Fig. 10**) [23].

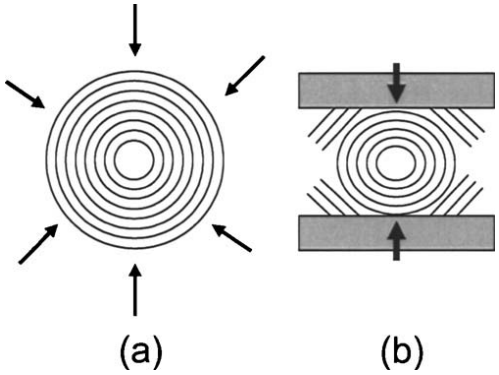

Figure 10. An MoS_2 nano-ball bearing two different forms of pressure: isotropic (a), normal stress (b) [23].

2.1.8 Tribological mechanisms

MoS_2 nanoballs have excellent lubricating properties as lubricating oil additives. There are three main frictional mechanisms that can explain this property: rolling, sliding, and exfoliation- transfer (third body) as shown in **Fig. 11** [24].

(1) Rolling: MoS_2 nano-balls roll as a ball bearing across frictional interfaces under relatively low normal stress. Roller is dependent on the shape of nano-balls which should be quasi-spherical structures.

(2) Sliding: Similar to nano-sheets, friction happens between external surfaces of the nano-balls under higher normal stress. The behavior of sliding is due to the shape of nano-MoS_2 particles, which is not perfectly spherical but of a faceted polyhedron structure. The corner of the faceted polyhedron structure can be easily distorted by asperities on the rough mating surfaces.

(3) Exfoliation and transfer (third body): Exfoliation is the main action of behavior under high normal stress resulting in deformation and even rupture of the nano-balls. Under the combined effects of the normal stress and shear stress, the external surface of the nano-ball particles can be exfoliated producing MoS_2 nano-sheets which can be adsorbed on the rubbing surfaces providing a protective layer and reduced the friction coefficient.

Among these three behaviors, rolling is generally accepted as the most prevailent mechanisms of friction reduction, motion because they cannot be detected directly only by micro frictional tests on the single MoS_2 nano-balls.

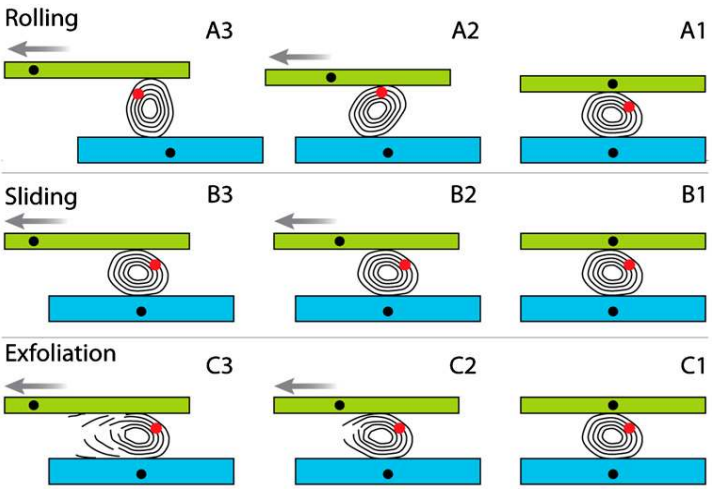

Figure 11. Schematic of the three main tribological mechanisms of MoS_2 nano-balls: rolling (A), sliding (B), and exfoliation and transfer (third body) (C) [24].

Particle size and crystalline perfection of the MoS_2 nano-balls are the most important factors that affect tribological behavior [6]. Generally, due to a nano bearing effect, the small MoS_2 nanoparticles have better antiwear and friction reducing properties than larger nanoparticles. However, with the decrease of particle size, the aggregation effects of the MoS_2 can increase and chemical stability reduces, which might result in reduced lubricity. Hence, particle size is very important in the efficacy of the additives. It is believed that exfoliation, rolling friction and third body transfer of MoS_2 sheets into surface asperities are the prevalent mechanisms that can explain the excellent tribological properties of MoS_2 nanoparticles [6].

There are no active dangling bonds in the closed-structure MoS_2 consequently, the oxidation temperature of MoS_2 nano-ball particles is ~100 ^{o}C higher than that of 2H-MoS_2. Moreover, under some testing conditions, the MoS_2 nano-ball particles had better lubricating properties than MoS_2 nano-sheets. This was ascribed to the chemical

stability of the layer-closed spherical structure of nano-balls. The detailed mechanisms for this are shown in **Fig. 12**. In air or when used in liquid paraffin nano-sheets, , due to the rim-edge site of the nano-sheets, they are easier to oxidized into MoO_3, there was a poor lubrication. MoS_2 nano-ball particles are relatively stable and can bear the shearing via rolling and elastic deformation.

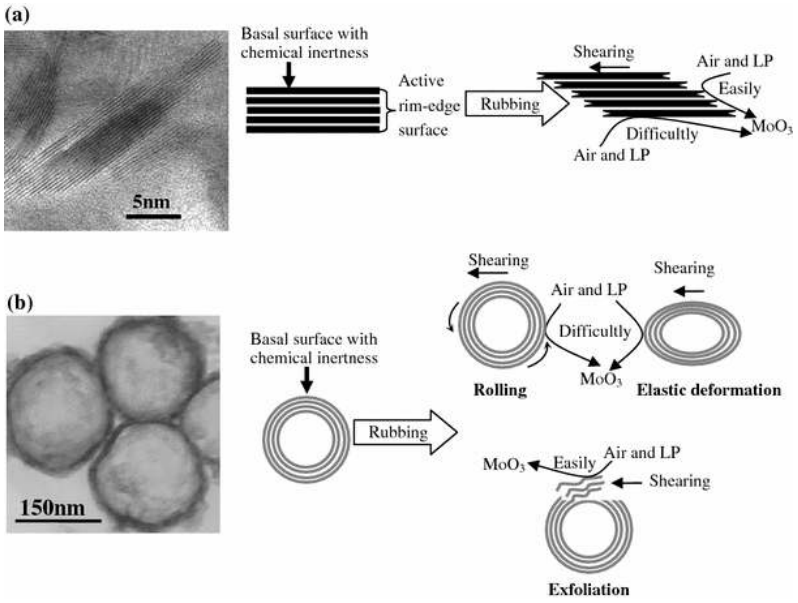

Figure 12. TEM images and schematics of the lubrication mechanisms of MoS_2 nano-slices (a) and MoS_2 nano-balls (b) [18].

2.2 MoS_2 nano-sheets

In recent years, the study of graphene-like two-dimensional layered materials has attracted great interest due to the successful exploration of graphene [25-27]. Among them, MoS_2 nano-sheets are the popular research molecular as a result of their distinct structure and superior properties. Functionalization, hybridization and modification of MoS_2-based nano-sheets has seen them used widely in various applications. Here, the preparation, characterization and properties of nano-sheets are reviewed.

2.2.1 Preparation of MoS_2 nano-sheets

It has been demonstrated that most of the methods for preparing 2-D nano-material such as graphene are effective for MoS_2 nano-sheets. The classic and straightforward way to prepare the nano-sheets is micro-mechanical cleavage [12]. Using this Top-down approach, a high-quality 2-D nano-material can be obtained [28]. However, the shortcomings of this method is also obvious. The productive efficiency is low and it is difficult hard to synthesize the 2D nano-sheets in large quantities. Moreover, the geometry can be very difficult to control precisely.

Ion-intercalation exfoliation is another popular method that can be used for preparation of MoS_2 nano-sheets. As shown in **Fig. 13**, there are three steps in this method : 1) introduction of Li^+ ions into the interlayer of bulk MoS_2; 2) immersion of Li_x-MoS_2 nano-sheets into water; and 3) ultrasonic processing of the solution.

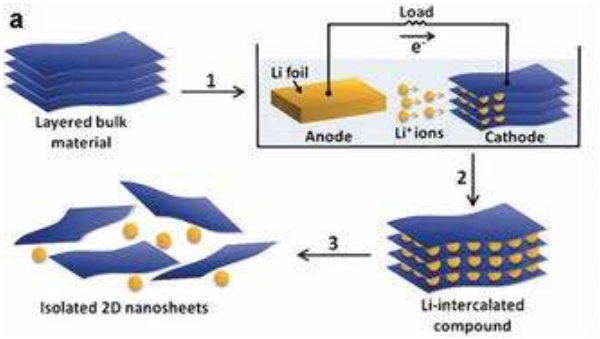

Figure 13. Schematic illustration of electrochemical lithiation and exfoliation process for the fabrication of 2D nano-sheets from layered bulk crystals [29] .

Bottom-up methods have been used to fabricate MoS_2 nano-sheets with desired size and thickness. Choudhary et al [30] adopted a sputter–chemical vapor deposition (CVD) technology to synthesize large-area, high-quality, and layer-controlled MoS_2 nano-sheets on a Si-based substrates. They also demonstrated that the single-layer MoS_2 over an area of 2 inch. with the domain size of 10–15 μm^2, showing good potential in future flexible, high-temperature, and radiation hard electronics/optoelectronics. Although CVD is an effective method for producing high-quality MoS_2 nano-sheets, there are some obvious disadvantages with the synthesis conditions, such as high temperatures, the requirement for a vacuum, and specific substrates, which restrict the practical applications of MoS_2 nano-sheets [31].

Owing to specific merits such as cheap raw materials, size and thickness controllable, high productive efficiency and no requirements on the substrates, solution-based methods have become prevalent in recent years. Smith et al [32] prepared MoS_2 nano-sheets through 1.5 mg mL^{-1} sodium cholate as a surfactant to exfoliate bulk MoS_2 in aqueous solutions. In a typical run, ultrasonic treatment can be used for the solution lasting 30 min, followed by centrifugation at 1500 rpm for 90 min.

2.2.2 Application of MoS_2 nano-sheets

One of the most important applications for MoS_2 nano-sheets is a substitute of noble metal catalysts such as Pt/C. It has been proved that the active edges of MoS_2 can be used as the active center for electro-catalysis [33]. Electro-catalytic perfor-

mance can be improved by reducing the dimension and by exposing the edges of the 2-D MoS_2.

Efficient energy storage is an important challenge for sustainable development. MoS_2 nano-sheets can be used in energy storage devices. One such application is in Li-ion batteries, which have been shown to be a highly efficient energy storage system. Although the charge capacity of the bulk MoS_2 is easy to reduce after use, after intercalating Li-ion into the interlayer of MoS_2, fewer layers of nano-sheets, the composites exhibited a high energy density capacity of 750 mA h g^{-1} even after 50 cycles [34]. Na ion intercalation in MoS_2 sheets has also shown promising results. Bang and his co-workers [35] reported a simplist method for enhancing the productive efficiency of MoS_2 nano-sheets in 1-methyl-2-pyrrolidinone with the assistant of sodium hydroxide. They also proved that at the high current densities, the exfoliated MoS_2 electrode exhibited better capacities than the pristine particle electrode (**Fig. 14**), indicating improved properties of the exfoliated MoS_2 nano-sheets with the reduced diffusion lengths of Na ions.

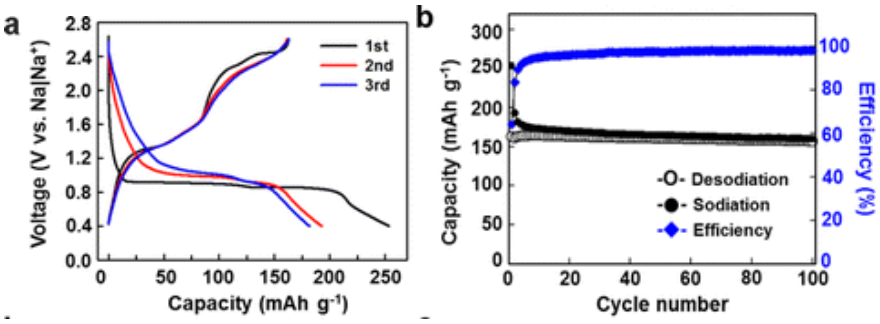

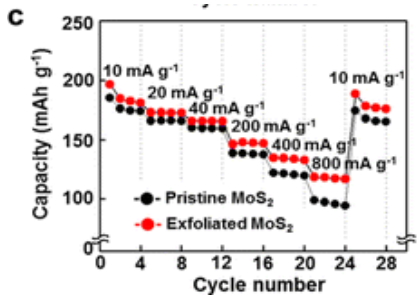

Figure 14. Charge–discharge curves (a) and the cycling properties and their coulombic efficiencies of the MoS_2 nano-sheets(b); the rate capability of pristine MoS_2 powder and the prepared MoS_2 nano-sheets at various current densities(c) [35].

Wu et *al.* [36] used electrochemically reduced single-layer MoS_2 nano-sheets for sensor applications. It was found that the prepared MoS_2 nano-sheets had good conductivity and high electrochemical sensitivity to detect glucose and biomolecules. Thus, reduced MoS_2 nano-sheets can be used in the development of novel electrode materials and can supply a novel platform for the sensing applications. Li et *al.* [37] used MoS_2 film-based field-effect transistors to detect NO at room temperature. The results showed that a single-layer MoS_2 nano-sheet had a rapid response to NO, but the current was unstable. A few-layer (less than 5) MoS_2 nano-sheet assembly presented both stable and sensitive responses to NO up to 0.8 ppm.

Another important application for MoS_2 nano-sheets is as lubricating additives. According to Wu et *al.* [38], with the addition of MoS_2 nano-sheets in liquid particles with concentration of 1.5 wt.%, the friction coefficients decreased significantly and are shown in **Fig. 15.** In addition, MoS_2 nano-sheets have a lower and more stable friction coefficient than commercial MoS_2 micro-particles with the size of 3–5 mm, owing to the surface effect just as can be seen graphene [39]. This can be explained

by the fact that MoS_2 nano-sheets have a larger surface area and higher chemical activity, which makes them easier to adsorb on to rubbing surfaces in the form of a stable tribo-film, reducing the friction and wear.

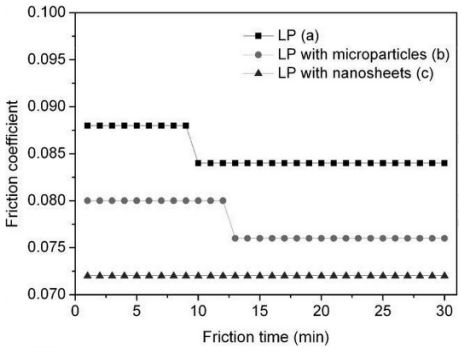

Figure 15. Friction coefficient of the base oil with different additives: Without additives (a), MoS_2 micro-particles (b) and MoS_2 nano-sheets (c) [38].

Hu et *al.* [40] prepared MoS_2 nano-sheets with thickness of 30-70 nm via a monolayer restacking process and studied tribological behaviors on a four-ball tribometer. Experimental results indicated that MoS_2 nano-sheets had better anti-friction, anti-wear and extreme pressure properties than micro-MoS_2 (**Fig. 16**). The excellent tribological properties of MoS_2 nano-sheets were attributed to a surface effect, dimension effect of the nanoparticles and a complex tribo-film composed of MoO_3 and $FeSO_4$ on the worn surfaces.

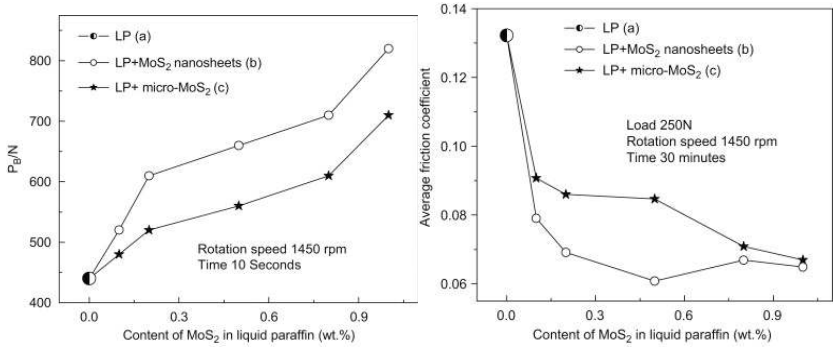

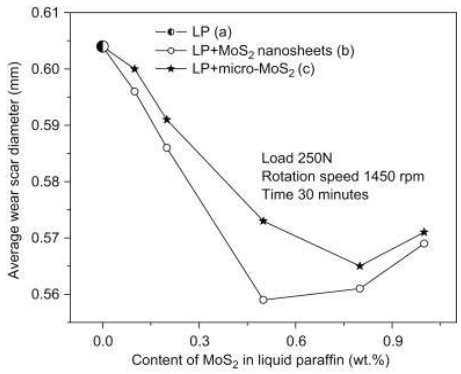

Figure 16. P_B values (a), average friction coefficient (b) and wear scar diameter (c) of liquid paraffin (a) with MoS_2 nano-sheets (b) and MoS_2 micro-sheets [40].

2.2.3 Tribological mechanisms of MoS_2 nano-sheets

As shown in **Fig. 17**, there are some S dangling bonds on the rim of MoS_2 nano-sheets. When they enter into frictional interfaces, MoS_2 nano-sheets could be adsorbed onto the frictional interfaces forming an adsorbed film depending on the formation of S-O or S-Fe bonds. The O and Fe came from the oxide layer on the surfaces of the substrate. The adsorbed film prevented frictional interfaces from direct contact and improved the tribological properties.

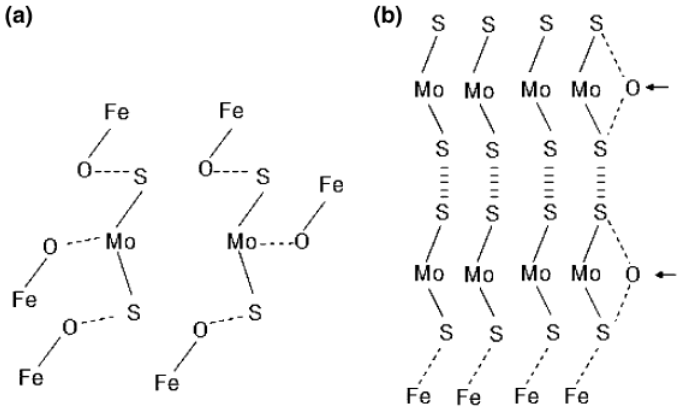

Figure 17. Schematic illustration of possible formation mechanisms of MoS_2 adsorbed film on iron oxide layer (a) and metal atom (b) [41].

Due to the chemical activity of dangling bonds, MoS_2 nano-sheets could be oxidized to MoO_3 and progressively sulfated, where oxygen might come from air or water during the sliding process. Fleischauer et *al.* [42] compared tribological properties of a typical MoS_2 film in which the sulfur was substituted for different contents of oxygen. They found that friction coefficient increased with increases in oxygen content at first, up a saturation point of 3% followed by a decrease. It is still higher than pure MoS_2 when oxygen content exceeded the critical value (**Fig. 18**).

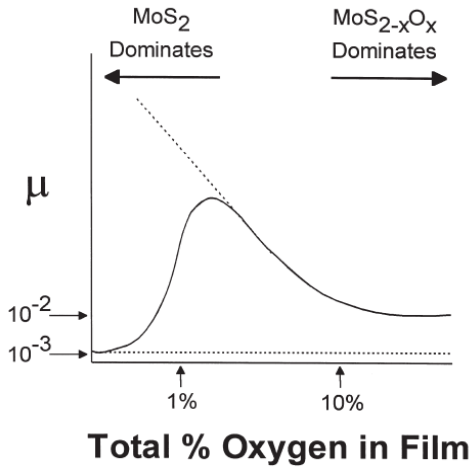

Figure 18. Variation of friction coefficient with the oxygen concentration in the film [42].

Onodera et al. [43] drew similar conclusions by simulating single sheet MoS_2 lubrication with computational chemistry methods. They proposed that the excellent tribological properties of MoS_2 sheets was attributed to the increase of coulombic repulsion energies between the two sulphur layers reacting with the iron surfaces as shown in the **Fig. 19.** With oxygen introduced into MoS_2, coulombic interaction energy reduced and roughness of MoS_2 layer increased. These resulted in the rising of the

friction coefficient. MoS_2 layers became flat again and decreased the friction coefficient with further increases in oxygen contents.

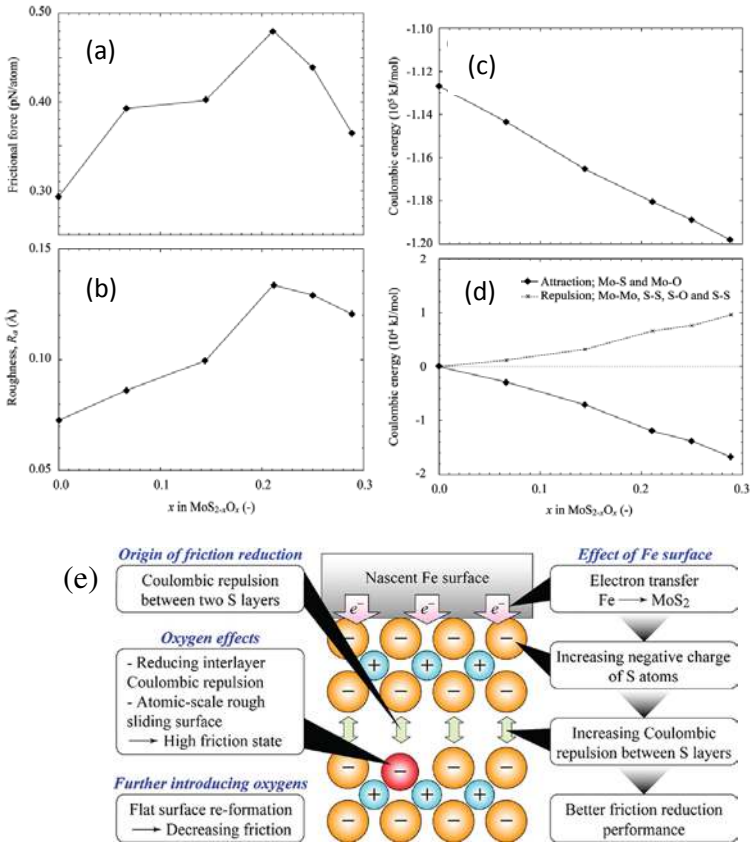

Figure 19. Average frictional force (a), Ra of top MoS_2 layer on sliding surface (b); total interlayer coulombic interaction energy (c); coulombic attractive and repulsive energies (d) along with oxygen concentration in MoS_2 structures; schematic illustration (e) for lubricating properties of MoS_2 single sheet [43].

2.3 MoS_2 nano-tubes

The MoS_2 nano-tubes, an analog of carbon nano-tubes, are considered to derive from lamellar compounds [44, 45]. The discovery of the carbon nano-tube has aroused great interest for the one-dimensional nano-tubes such as MoS_2 due to their

small dimensions, high anisotropy, and special tube-like structures [46]. In this section, the preparation, characterization and application of MoS_2 nano-tube will be described and discussed.

2.3.1 Preparation, Characterization of MoS_2 nano-tube

Remskar et *al.* [46] used 5 wt % C_{60} as a catalyst during the production process. In a typical run, the reaction conditions were controlled as follows: reaction time: 22 days; temperature: 1010 K; reactor: silica ampoule; pressure: 10^{-3} Pa. The SEM and TEM images of the nano-tubes are shown in **Fig. 20**. The conversation rate was about 15% for MoS_2 nano-tubes.

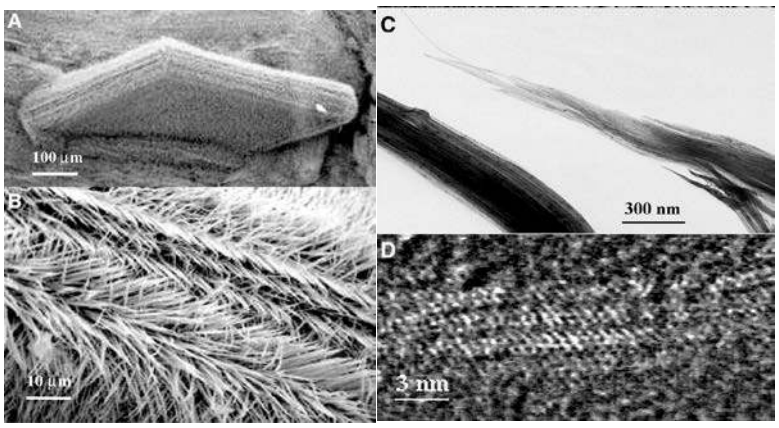

Figure 20. SEM and TEM images on different length scales. (A) Bundles appear to self-assemble into various different microscopic structures. (B) The bundles end in sharp points. (C) A split tip of a bundle terminating in strands ~4 nm wide. (D) Expanded electron transmission view of a strand composed of an only few individual nano-tubes [46].

Template synthesis is another path to obtain MoS_2 nanotubles. Zelenski et *al.* [47] used aluminum oxide templates to prepare near-mono dispersed MoS_2 nano-tubules.

As shown in **Fig. 21**, the fibers in the picture were synthesized in 0.1 M $(NH_4)_2MoS_4$ DMF solutions. They were separated from the template by the dissolution of the template using 1.0 M NaOH solutions. Fig. 21b presents an end-on view of the nano-tubes and confirms their hollow nature.

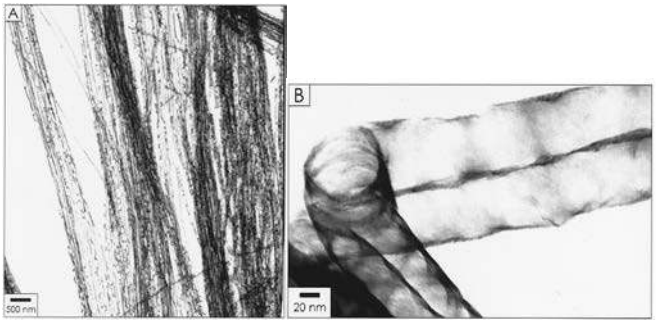

Figure 21. A TEM image of the MoS_2 tubes after dissolution of the aluminum oxide template (A). A TEM image of a bend in a tubule of MoS_2 emphasizing the hollow nature of the tubules (B) [47].

Nath et al. [48] developed a simple synthesis method of MoS_2 and WS_2 nano tube. The first step was to prepare MoS_3 precursors via decomposition of $(NH_4)_2$ MoS_4 at 400 ^oC in an argon atmosphere. Then, the precursors were heated at 1200-1300 ^oC under H_2 atmosphere. MoS_2 nano-tubes were formed, and the TEM images are shown in **Fig. 22**. It can be seen that the external diameter of the nano-tube is about 20-30 nm, and the wall thickness is about 10-15nm. There are also some onion-like clusters in the Figure, suggesting the existence of an intermediate stage between MoS_3 precursors and MoS_2 nano-tubes [49]. Feldman et *al.* [50] used the gas-phase reaction between MoO_3 and H_2S in a reducing atmosphere at high temperature and also got high-rate growth of MoS_2 nano-tubes.

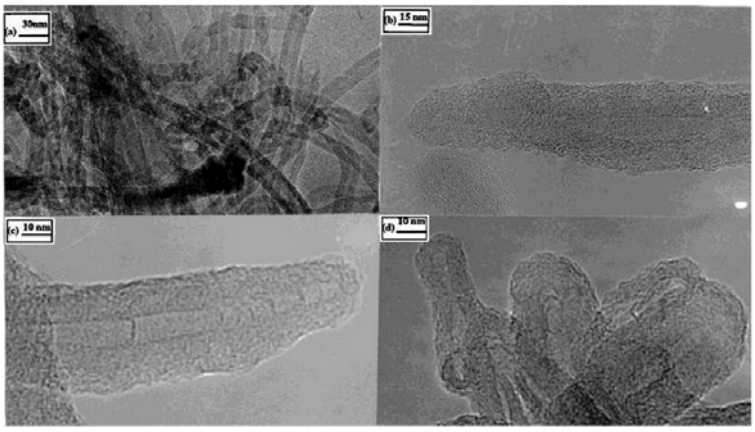

Figure 22. TEM images of MoS_2 nano-tubes: (a) Images of several nano-tubes; (b) and (c) high resolution images of the nano-tubes; and (d) nested-shell and onion-like clusters with hollow core [48].

2.3.2 Applications of MoS_2 nano-tubes

Besides the synthesis and characterization of MoS_2 nano-tubes, studies have been focused on a great number of particular properties and applications [51], for instance, mechanical properties [52], field emission properties [53], in hydrogen storage applications [54] and as catalysts [55].

Chen et al. [55] synthesized an open-ended MoS_2 nano-tube and used it as the catalyst of methanation of CO and H_2 at relatively low temperatures (**Fig. 23**)). Techniques such as this contributes to new ways of reducing the environmental load resulting from CO emissions. By analyzing the shear and Young's moduli of the MoS_2 nano-tubes, Kis et al. [56] used an atomic force microscope to study the interaction between the MoS_2 nano-tubes, finding the MoS_2 nano-tube ropes were highly anisotropic and very weak.

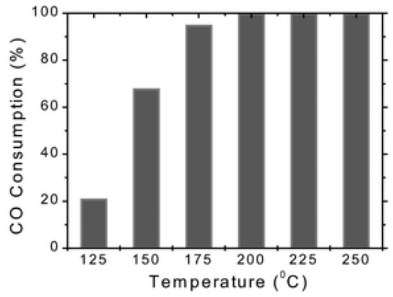

Figure 23. Catalytic abilities of MoS_2 nano-tubes [55].

Chen et al. [44] prepared MoS_2 nano-tubes by heating $(NH_4)_2MoS_4$ in hydrogen/thiophene. They studied the electrochemical properties. It was found that the highest capacity was 260 mAh g^{-1} because of a highly nano-porous structure, suggesting a potential application in electrochemical catalysis and high-energy batteries.

Analogouslyto MoS_2 nano-tube, WS_2 nano-tubes, can be used for tips in scanning-probe microscopy [57]. They have been successfully applied in the inspection of microelectronics circuitry. With improvements in productity for producing these, the application of MoS_2 nano-tubes will widen to include nanolithography, photocatalysis, sensors and others [58].

MoS_2 nano-tubes also have excellent lubricating properties whether as lubricating oil additives or prepared as self-lubricating composite materials [59, 60]. However, due to their thin and long structure and chemical inertness, MoS_2 nano-tubes are hard to disperse in lubricating oil which limit their tribological application. Modification, treatment or the addition of a dispersion agent is an effective method to improve dispersion in oil of nano-tube[61, 62]. Kalin et *al.* [63] investigated the frictional properties of MoS_2 nano-tubes as oil additives. They found that the lubrication mechanism

was mainly exfoliation and deformation which was similar to that of MoS_2 nanoballs. Exfoliated nano-sheets were adsorbed on to the rubbing surfaces, and compacted and deformed to form a boundary film. With these two combined effects, MoS_2 nano-tubes reduce friction and wear significantly.

3. Graphene and its tribological applications

Graphene, just like the structured MoS_2, is a 2-D layered material with sp^2-bonded carbon, that has received substantial attention [64-66] due to its good conductivity, excellent mechanical properties, potential applications in electrochemical energy storage [67], microelectronics and lubricating additives [68, 69]. In this section, the preparation, characterization and applications of graphene is reviewed to give a view on the increasingly wide scope of applications.

3.1 Preparation and characterization of Graphene

Graphene was firstly prepared by Geim et al. at the University of Manchester in 2004 by using tape [70]. This was work for which they were awarded the Nobel Prize in Physics in 2010. From this point, graphene has attracted substantial research attention such that it's synthesis, characterization, its unique structures and superior properties are well studied

3.1.1 Exfoliation in liquid or gas

Exfoliation of graphite in liquid or gas is physical method to obtain graphene. Hernandez et al. [71] demonstrated that dispersion and exfoliation of graphite in N-methyl-pyrrolidone to obtain graphene blended solutions with a concentration of 0.01 mg ml^{-1}. However, the yield of single-layer graphene was low at about 1%.

3.1.2 Modified mechanical exfoliation

Recently, in order to improve the yield of production of single layer graphene, Xu et al. [72] used a friction-induced exfoliation from graphite to graphene in esterified bio-oil. They dispersed flake graphite into the esterified bio-oil and then measured the tribological response of the dispersed graphene after ultrasonication for 20 min. Testing was performed on a ring-on-plate tribometer. It was found that both load and sliding speed had an important effect on the quality of the graphene. Higher loads and lower sliding speed were helpful to form the single-layer graphene. In addition, higher loads also contributed to friction and wear reduction in the tribosystem due to the formation of a thicker tribofilm.

3.1.3 Epitaxial growth

Due to the low efficiency of the mechanical exfoliation method, epitaxial growth has become one of the most important methods to produce the graphene film on certain substrates such as SiC and transition metals [73]. Yang et al. [74] used a plasma-assisted deposition epitaxial growth method to obtain the single-domain graphene on hexagonal boron nitride. The graphene was produced at ~500 °C. A schematic illus-

tration of this process is shown in **Fig. 24**, suggesting a typical edge growth of carbon atoms. The sp^2 carbon structure of the graphene were confirmed by Raman spectra in Fig. 24b. The AFM images also showed the existence of single layer graphene.

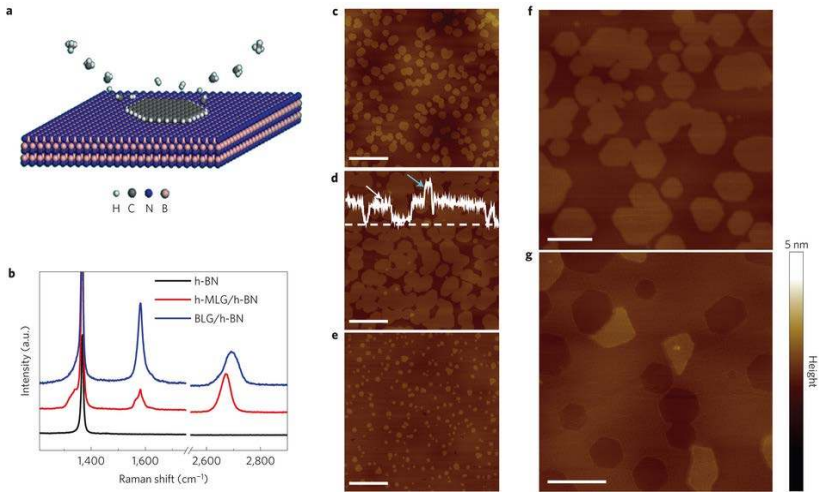

Figure 24. Schematic illustration of the growth mechanism (a); Raman spectra for hexagonal MLG (h-MLG) grains (red), BLG film (blue) and bare h-BN surface (black) (b). c–e, AFM images of as-grown graphene on h-BN at different stages including small grains nucleation (c), coalescence of grains (d), and continuous monolayer graphene with some second-layer nuclei on top. A height profile was extracted along the dashed white line cut in d, with white and cyan arrows indicating the first and second layer, respectively. The scale bars in c–e are 500 nm. f, g, Zoom-in AFM image of as-grown graphene showing aligned hexagonal grains (f) or pits after plasma etching (g). The scale bars in f, g are 200 nm [74].

Fumihiko et al. [75] grew graphene on a SiC (0001) substrate under the temperatures varying from 600 to 915 °C by thermal decomposition of a cracked-ethanol source. This is an example of one kind of gas-source molecular beam epitaxy (MBE)

methods. The experimental results showed that higher temperatures were helpful to prepare high quality single-layer graphene. Unfortunately, the growth rate decreased with the increase in temperatures. Moreover, there was a network of fin-like ridge shapes of graphene (**Fig. 25**).

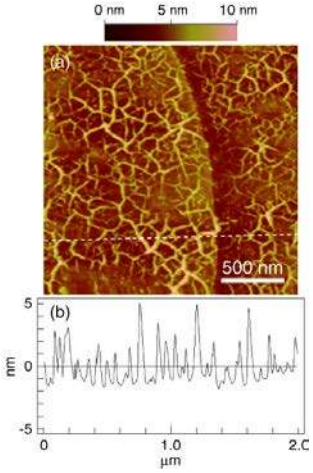

Figure 25. Topographic AFM image of graphene (a), and the height of the line in the AFM image (b) [75].

However, the epitaxial growth method for producing graphene has some disadvantages. For instance, it requires some harsh conditions, including high temperature, high vacuum, special atmosphere and substrates. The synthesized graphene is also hard to separate from the substrate. It is also hard to produce graphene on a large scale in industry.

3.1.4 Chemical vapor deposition

Chemical vapor deposition (CVD) has been used to produce high-quality thin films on substrates in the semiconductor industry. In recent years, this technique has

also been applied to synthesis graphene. The principle is to deposit volatile precursors onto the substrate.

A single- and few-layer (less than 10) graphene film with large area (~ cm^2) was prepared by Reina et al. over an Ni surface using CVD technology [76]. But the lateral size was limited to 20 μm. The domain boundaries have proved adverse to the transport properties. Thus, graphene with a larger area is still the pursuit of the scientists. Li et al. [77] prepared single crystal graphene with domain size of up to 0.5 mm (**Fig. 26**), which were grown at low-pressure and high-temperature chemical vapor deposition (8 mTorr at 1035 °C) on copper-foil enclosures using methane as a precursor. The flow rates and partial pressures of the methane were less than 1 sccm and 50 mTorr, respectively. The transport properties of the graphene film were measured, and the mobility of the films was found to be a little bit higher than 4000 $cm^2\ V^{-1}\ s^{-1}$, indicating further improvements for this graphene film should be possible.

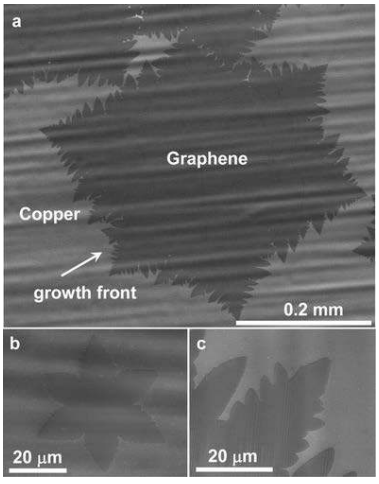

Figure 26. SEM images of graphene on copper grown by CVD: Graphene domain grown at 1035 °C on Cu at an average growth rate of ~6 μm/min (a). Graphene nuclei formed during the initial stage of growth (b). High-surface-energy graphene growth front (c) [77].

CVD methods can produce high-quality graphene with large area, with the products easily separated or transferred from substrates. In addition, CVD derived graphene can be processed at relatively low temperatures and ambient pressure. However, the thickness of the graphene is hard to control and the yield remains low.

3.1.5 Reduced graphene oxide

A reduced graphene oxide method for the production of graphene in aqueous solution has attracted great interests due to its low cost, easy processability and high efficiency. The process includes three steps: 1) preparation of oxide graphite from graphite using strong oxidants such as concentrated sulfuric acid, concentrated nitric acid and potassium permanganate; 2) ultrasonic process for separating the lattices of oxide graphite; 3) reduction of the graphene oxide with reducer such as hydrazine hydrate and sodium borohydride.

Tkachev et al. [78] used a modified Hummers method to prepare graphite oxide, and then synthesized the graphene oxide by ultrasonic processing. The final reduced graphene oxide was obtained after the appropriate amount of graphene oxide and ethanol were mixed and reacted at 200–380 °C for 10–90 h. A typical detailed process for preparing reduced graphite oxide is shown in **Fig. 27**.

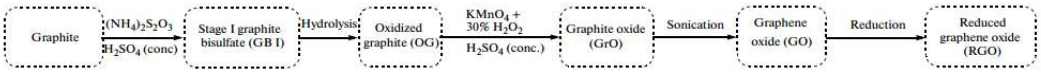

Figure 27. The preparation process of reduced graphene oxide [78]

3.2 Properties and applications of graphene

Graphene has become a star molecule over the last c.10 years because of the ability to its particular structure and properties such as electrochemical, mechanical and other properties. The progress of the main properties of graphene is reviewed in this section.

3.2.1 Electrochemical properties

Electrons in graphene have a character that can be described by a linear dispersion relationship. It has been confirmed that at room temperature the electron mobility of single-layer graphene amounts to $15,000\ m^2\ V^{-1}\ s^{-1}$. Therefore, graphene has many potential applications in microelectronic devices [79]. Geim et al. [79] noted that the conductivity of graphene was much higher than that of single-walled carbon nano-tubes by about 60 times. In addition, they found that graphene had higher surface negative charge, better stability and signal-to-noise ratio than single-walled carbon nano-tubes, indicating the potential of graphene in the detection of some small molecules such as dopamine and serotonin by graphene electrodes.

Shan et al. [80] used graphene to increase the conductivity and electrochemical stability of MoS_2 since MoS_2 has a high theoretical specific capacity (about 670 $mA\ h\ g^{-1}$) but low cycle charging performance. A unique film–foam–film structure was designed to solve this problem. The experimental results showed that the appropriate structures resulted in a high, reversible Li storage capacity of 1200 $mA\ h\ g^{-1}$

and a longer lifetime, suggesting its potential application in high-energy-density batteries.

3.2.2 Mechanical properties

With the potential application of graphene in nanoelectromechanical systems, the mechanical properties of mono-layer or few-layer graphene (less than 5) have aroused great interest. Frank et al. [81] used an atomic force microscope to measure the effective spring constants of the graphene sheets with thickness between 2 to 8 nm ranging from 1 to 5 N m^{-1} and the Young's modulus of graphene sheets is 0.5 TPa, which is a half of bulk graphite.

Young's modulus was studied by molecular dynamics and was predicted higher than 1 TPa [82]. According to Lee et al. [83, 84], the Young's modulus and fracture strength of a defect-free graphene were 1.0 TPa and 130 GPa, respectively, being measured by an AFM indentation approach (**Fig. 28**).

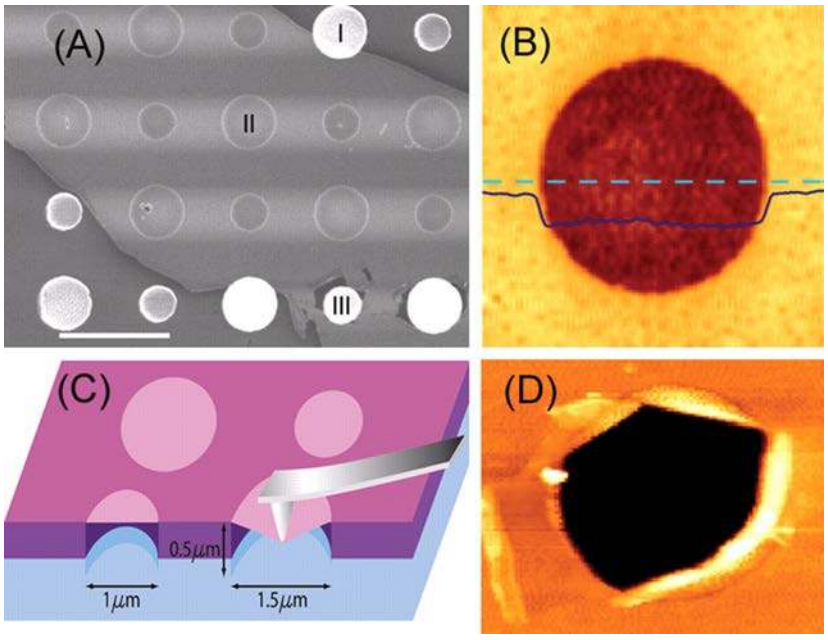

Figure 28. Images of graphene membranes: SEM images of a large graphene flake spanning an array of circular holes 1 μm and 1.5 μm in diameter. Scale bar, 3 μm (A). Noncontact mode AFM image of one membrane (B). Schematic of nanoindentation on suspended graphene membrane (C). AFM image of a fractured membrane (D) [84].

3.2.3 Optical properties

Of main interest for graphene is the comparison of the permittivity features. Falkovsky [85] investigated the transmittance of graphene in the optical region and found that optical properties were affected by the interband electron transitions. Moreover, the transmittance of graphene in the visible spectrum range was not affected by frequency and had a constant value depending on its fine structure.

3.2.4 Extreme pressure properties

The extreme pressure value (P_B) of oil is an important parameter when evaluating the load carrying capacity of lubricating oil. Nano scale lubricating particles being mixed with oil can penetrate into rubbing surface during sliding and protect rubbing surfaces from contacting directly and can form an adsorbed layer. Because of the excellent anti-wear properties, nanoparticles with a low concentration can improve P_B values significantly. As shown in **Fig. 29**, comparing with the base oil or base oil with flake grphite, MoS_2 nano-sheets and graphene can increase P_B value to approximately 2 and 1.6 times, respectively at optimum concentrations [40, 86].

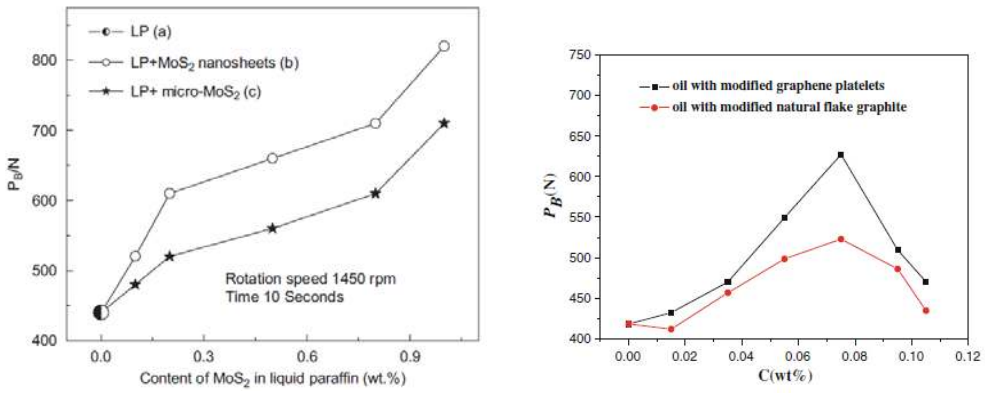

Figure 29. Effect of concentration of MoS_2 nano-sheets (left) [40] and graphene (right) on the P_B value [86].

3.2.5 Dispersion properties

The advantage of nanoparticles is that they can penetrate into mating surfaces during frictional process even in severe boundary lubrication. However, nanoparticles tend to agglomerate due to nanometric size effects. The size of the agglomeration might amount to a few microns which make the particles much less likely to penetrate into frictional interfaces, and so the cannot reduce the friction and wear of the tribosystem. Therefore, the dispersive properties of the nano-lubricating additives are very important. Modification treatments are a chemical reaction method to graft a modifier on the nanoparticles to improve the dispersive properties. The modifiers commonly have an oleophylic functional group of long chain alkane. Although graphene has excellent tribological properties, the dispersion of graphene in oil is poor which leads to coagulation and precipitation of graphene quickly because of chemical inertness.

Modifying graphene with an appropriate modifier is an effective approach to forming stable dispersions and preventing aggregation. Lin et al. [86] modified graphene by using stearic and oleic acids. The modifiers, cyclohexane and dried graphene were heated and stirred at 80 °C for 5 h. There was some residual oxygen-containing functional groups, as a result of the incomplete diminution of reduced graphene oxide, that could react with carboxyl groups of stearic and oleic acids. Therefore as a result of the long chain molecular structures of stearic and oleic acids, modified graphene has better dispersive properties than the pristine graphene as shown in **Fig. 30.**

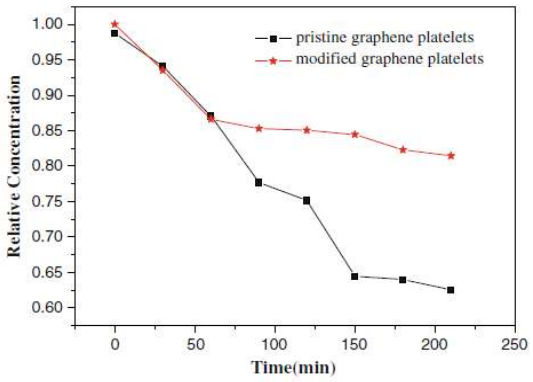

Figure 30. Dispersive stability of graphene in lubricating oil [86].

3.2.6 Tribological properties and applications of graphene

Graphene has excellent tribological properties as lubricating oil additive in part due to its layered structure similar in many respects to MoS_2,. Eswaraiah et al. [87] synthesized ultrathin graphene with thickness of ~2 nm via reducing graphene oxide with focused solar radiation. The tribological properties were investigated by using a four-ball tribometer. They found that the ultrathin graphene dramatically reduced av-

erage coefficient friction and wear loss at relative low concentration in a formulated engine oil as shown in **Fig. 31**. Also graphene can significantly improve the load capacity of a lubricant owing to its excellent anti-wear performances especially at concentration of 0.025 mg mL^{-1}. In addition, graphene in the base oil could be adsorbed on the frictional interfaces and by forming a physically adsorbed film. The adsorbed film protected the rubbing surfaces and reduced wear and the coefficient of friction.

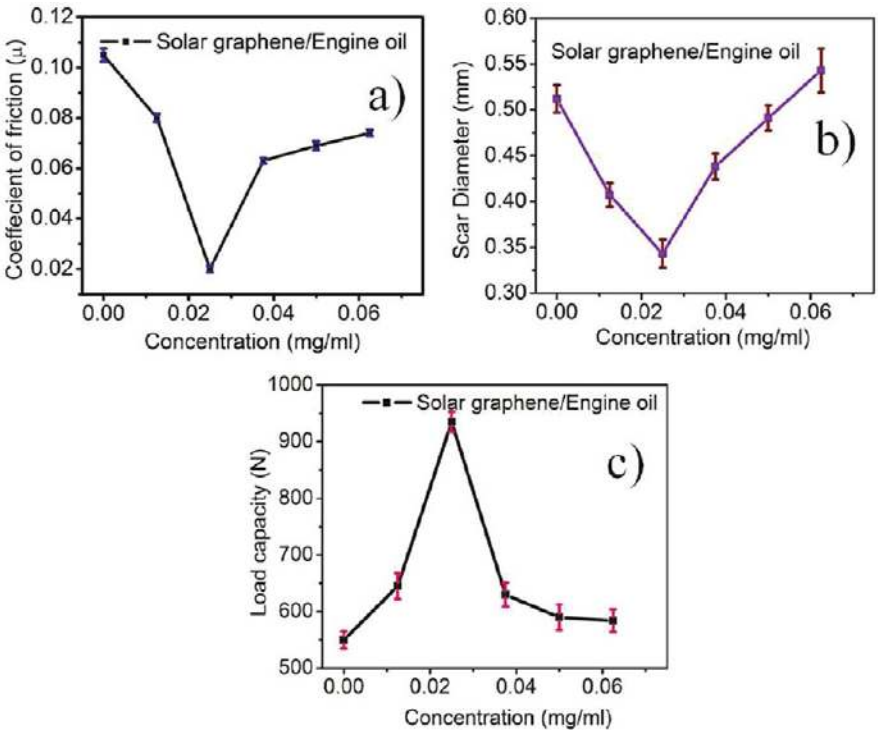

Figure 31. Tribological properties of graphene dispersed in engine oil: Coefficient of friction (a), wear scar diameter (b), and load capacity (c) [87].

According to the results in **Fig. 31**, graphene has an optimal concentration. The antifriction and antiwear behaviors deteriorated when the concentration of graphene exceeded the optimal concentration. This can be explained by the fact that graphene can form an adsorbed film protecting frictional interfaces at an optimal concentration.

However, when the concentration exceeded the critical value, the lubricating oil in the friction region is reduced by the aggregation of graphene, which makes the oil film discontinuous and reduces the lubricating effects. The corresponding lubrication mechanisms of graphene as an oil additive in different lubricating state are shown in **Fig. 32** [88].

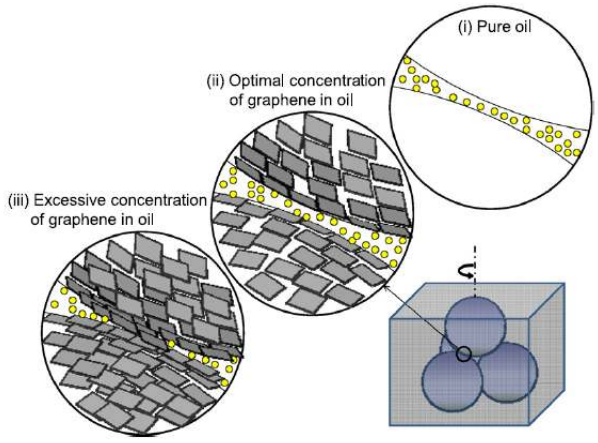

Figure 32. Schematic of the lubrication mechanisms of graphene as oil additives at different lubricating states [88].

4. Synergistic lubricating behaviors of graphene and MoS_2

Previous studies [89-95] have shown that the tribological mechanisms of MoS_2 are interlayer slippage, rolling deformation, and a slippery exfoliation. But the MoS_2 particles are easily removed during frictional process, which affects their long-term effects. Considering good adhesive and lubricating properties of graphene [96-100], the joint use of graphene and MoS_2 seems to be a good choice. Currently, graphene/MoS_2 composites have been selected as a photoresponsive coating [101], electrochemical sensors [102], catalyst supports [103] and for lithium storage [104]. Xu et

al. [105] have systematically studied the lubricating properties of graphene/MoS_2 composites, the results and tribological mechanisms are reviewed in detail in the following sections.

4.1 Tribological behaviors

Tribological tests were performed on a four-ball tribometer. The dispersive media was bio-oil and detailed frictional conditions were as follows: concentration of the additives: 0.5 wt.%; Load:300 N; Rotating speed: 1000rpm; Sliding time: 30min. As shown in **Fig. 33**, the MoS_2/graphene composite had a lower friction coefficient and wear loss including wear scar diameter (WSD) and wear scar width (WSW) than MoS_2 or graphene. This suggested a clear synergistic lubricating role of graphene/MoS_2 composites.

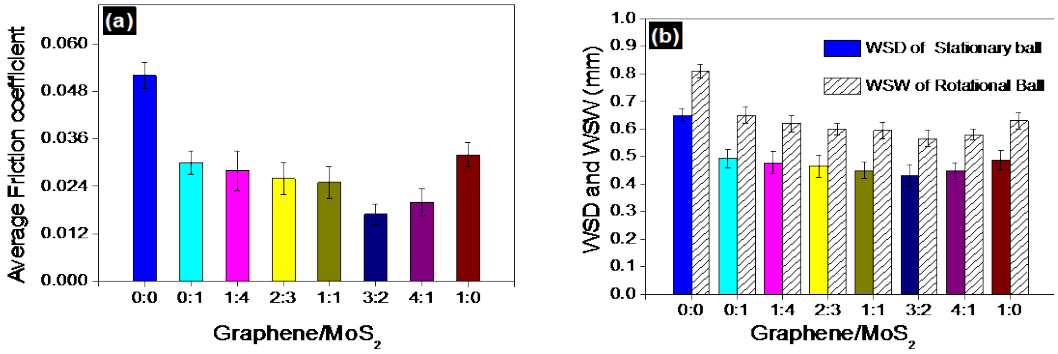

Figure 33. Average friction coefficient (a) and WSD and WSW (b) of graphene and MoS_2 dispersed in base oil with different mass ratio [105]

The effect of the loads on the tribological behavior of the graphene/MoS_2 composite is shown in **Fig. 34**. The friction coefficient, WSD and WSW of pure base oil

and esterified bio-oil (EBO), increased with load, due to the smaller micro-intervals between the friction pairs under higher loads [106]. There was a great decrease in the friction coefficient and wear loss of the EBO with graphene/MoS_2 composite additives, up to 300N. Exceeding this load, the friction coefficient and wear loss remained stable or increasing. At the same time, for the same load, the EBO with graphene/MoS_2 composite additives showed the best lubricity in all the four lubricants. This confirms the synergistic lubricating effects between graphene and MoS_2.

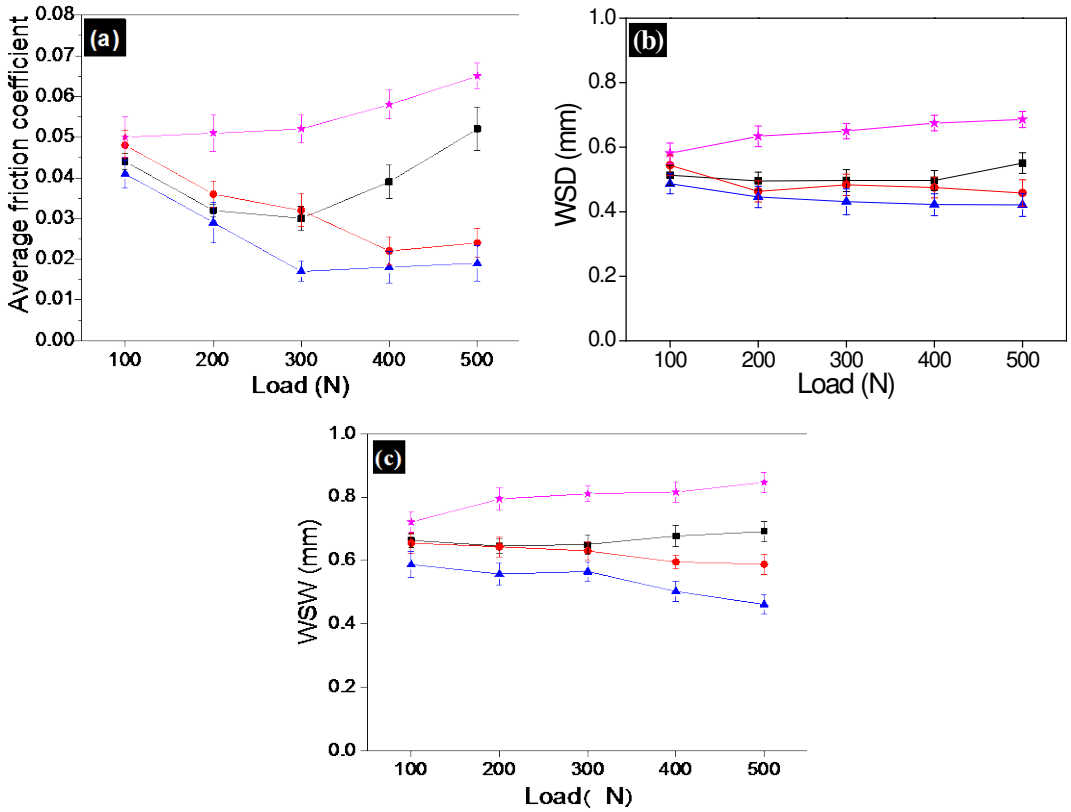

notes: ★ EBO; ● EBO+0.5 wt.% graphene; ■ EBO+0.5 wt.% MoS_2; ▲ EBO+0.3 wt.% graphene+0.2 wt.% MoS_2

Figure 34. Average friction coefficient (a), WSD (b) and WSW (c) of steel specimens under different loads [105].

4.2 Friction and wear mechanisms

In order to explore the friction and wear mechanisms of the graphene/MoS_2 composites, XPS spectra of the typical elements on the rubbed surfaces are shown in **Fig. 35.** The position of the two C1s peaks suggested the existance of carbon or sp^3 C (C–C/C–H) and sp^2 C (C=C/C=O) [107], respectively. This indicated that the adsorbed film was made from carbon or organics, coming from the graphene or base oil. The largest areas of C1s peaks of graphene/MoS_2 blends suggested the formation of the thickest adsorbed film containing graphene and organics. The O1s peak can be ascribed to hydroxides or sulfates, confirming the existence of an adsorbed film with organics or a tribo-film with sulfates. The O1s peak at 530.3 eV was attributed to Fe_2O_3, suggesting the tribo-oxidation of the substrate during sliding. The Fe2p peaks belonged to Fe_2O_3, and no simple Fe^0 peak was found, confirming the existence of a complete tribo-oxide film on the rubbing surfaces. The Cr2p peaks belonged to Cr_2O_3 and CrN, respectively. This confirmed a tribo-oxidation and tribo-reaction during the sliding process.

For graphene/MoS_2 lubrication, the two main Mo3d peaks at 232.6 and 235.8 eV were ascribed to MoO_3 [9]. Another peak at 229.7 eV was ascribed to Mo3d of MoS_2, but this peak was not detected for MoS_2 lubrication. Moreover, the two S2p peaks at 169 eV and 161.6 eV were indexed to SO_4^{2-} and MoS_2, respectively [108]. When MoS_2 was used independently (c), the peak at 161.6 eV in the curve was very weak, suggesting that MoS_2 was easily oxidized during sliding. That is, the introduction of graphene was helpful to the adhesion of the MoS_2 on the frictional surface and further prevents the oxidation of MoS_2.

The friction and wear mechanisms were summarized as follows. For graphene, the main antifriction and antiwear components were the small graphene particles, and ploughing was the dominant form of wear. For MoS_2, the MoS_2 with smaller surface area was the main lubricant but it is easily to be removed from the frictional surface or oxidized. For graphene/MoS_2 composites, a thicker tribo- film was formed to play an antifriction and antiwear role. The synergistic lubricating effect of graphene and MoS_2 allows complete graphene and unoxidized MoS_2 to remain on the sliding surfaces.

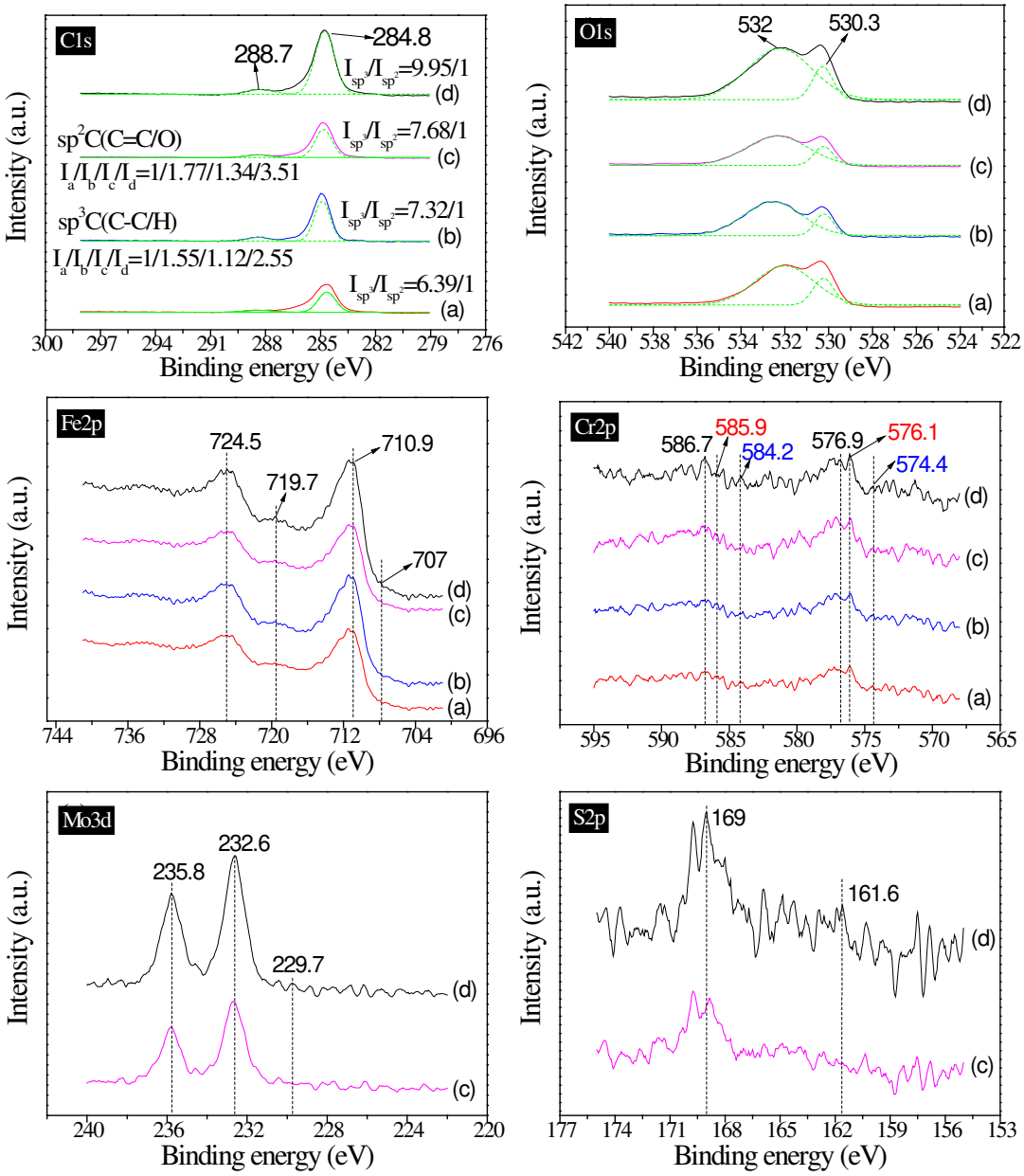

Figure 35. XPS spectra of the worn surfaces on the rotating specimen lubricated by base oil (a), base oil with graphene additives (b), base oil with MoS_2 additives (c), base oil with graphene/ MoS_2 composite additives (d) [105].

5. Conclusions

In summary, in this chapter, two kinds of nano additives MoS_2 and graphene have been reviewed. The preparation methods, properties and applications have also been discussed. Both MoS_2 and graphene have various functions and applications and their tribological properties have been explored this chapter. For MoS_2, different structures have different physical properties. Nano-MoS_2 showed obvious advantages over the more conventional micro-MoS_2. In a widely accepted opinion, rolling is the main antifriction and antiwear mechanism for nano-MoS_2 particles. The slippery role is the friction-reducing mechanism of MoS_2 nano-sheets and the combined actions of rolling and sliding account for the excellent lubricating effect of MoS_2 nano-tubes. However, exfoliation and transfer cannot be ignored when explaining the tribological behaviors of nano-MoS_2. More combined applications of nano-MoS_2 with different structures requires further study.

As for graphene, good adsorption onto the frictional surfaces is helpful to the lubricating behaviors of graphene. However, the effects of the layer, area and defects inthe graphene on the tribological behaviors still remain unknown and need further clarification in the future. The graphene/MoS_2 composites showed excellent synergis-

tic lubricating effect. The mechanisms were attributed to the protective roles of the graphene preventing the oxidation of MoS_2 and also MoS_2 preventing graphene being destroyed and reduced into small, defective additives. The MoS_2 used in the composites was micro-MoS_2, nano-MoS_2 composites needed to be studied further. To conclude, both graphene and MoS_2 as lubricating additives have a bright future and more specialized applications will be researched and found.

Acknowledgements:

This work was supported by the National Natural Science Foundation of China (Grant No. 51405124), the China Postdoctoral Science Foundation (Grant Nos. 2015T80648 & 2014M560505), the Anhui Provincial Natural Science Foundation (Grant No. 1408085ME82) and the Tribology Science Fund of State Key Laboratory of Tribology, Tsinghua University (Grant No. SKLTKF15A05). In the UK, the research was supported by the Engineering and Physical Sciences Research Council, grant number EP/L017725/1.

References:

[1] L. Price, M.D. Levine, N. Zhou, D. Fridley, N. Aden, H. Lu, M. Mcneil, N. Zheng, Y. Qin, Y. Ping, Assessment of China's energy-saving and emission-reduction accomplishments and opportunities during the 11th Five Year Plan, Energ. Policy 39 (2011) 2165-2178.

[2] E.A. Abdelaziz, R. Saidur, S. Mekhilef, A review on energy saving strategies in industrial sector, Renew. Sust. Energ. Rev 15 (2011) 150-168.

[3] B. Zhmud, B. Pasalskiy, Nanomaterials in lubricants: an industrial perspective on current research, Lubricants 1 (2013) 95-101.

[4] R.G. Dickinson, L. Pauling, The crystal structure of molybdenite, J. Am. Chem. Soc. 45 (1923) 1466-1471.

[5] M. Ye, D. Winslow, D. Zhang, R. Pandey, Y.K. Yap, Recent advancement on the optical properties of two-dimensional molybdenum disulfide (MoS_2) thin films, Photonics, Multidisciplinary Digital Publishing Institute, 2015, pp. 288-307.

[6] R. Rosentsveig, A. Gorodnev, N. Feuerstein, H. Friedman, A. Zak, N. Fleischer, J. Tannous, F. Dassenoy, R. Tenne, Fullerene-like MoS_2 nanoparticles and their tribological behavior, Tribol. Lett. 36 (2009) 175-182.

[7] H.D. Huang, J.P. Tu, T.Z. Zou, L.L. Zhang, D.N. He, Friction and wear properties of IF–MoS_2 as additive in paraffin oil, Tribol. Lett. 20 (2005) 247-250.

[8] K.H. Hu, Y.R. Wang, X.G. Hu, H.Z. Wo, Preparation and characterisation of ball-like MoS_2 nanoparticles, Mater. Sci. Technol.-lond. 23 (2007) 242-246.

[9] K.H. Hu, J. Wang, S. Schraube, Y.F. Xu, X.G. Hu, R. Stengler, Tribological properties of MoS_2 nano-balls as filler in polyoxymethylene-based composite layer of three-layer self-lubrication bearing materials, Wear 266 (2009) 1198-1207.

[10] I. Lahouij, B. Vacher, F. Dassenoy, Direct observation by in situ transmission electron microscopy of the behaviour of IF-MoS_2 nanoparticles during sliding tests: influence of the crystal structure, Lubr Sci 26 (2014) 163-173.

[11] Y. Li, H. Wang, L. Xie, Y. Liang, G. Hong, H. Dai, MoS_2 nanoparticles grown on graphene: an advanced catalyst for the hydrogen evolution reaction, J. Am. Chem. Soc. 133 (2011) 7296-7299.

[12] B. Radisavljevic, A. Radenovic, J. Brivio, i.V. Giacometti, A. Kis, Single-layer MoS_2 transistors, Nat. Nanotechnol. 6 (2011) 147-150.

[13] S. Aralihalli, S.K. Biswas, Grafting of dispersants on MoS_2 nanoparticles in base oil lubrication of steel, Tribol. Lett. 49 (2013) 61-76.

[14] J.D. Desai, I.M. Banat, Microbial production of surfactants and their commercial potential, Microbiol. Mol. Biol. Rev. 61 (1997) 47-64.

[15] A. Moshkovith, V. Perfiliev, I. Lapsker, N. Fleischer, R. Tenne, L. Rapoport, Friction of fullerene-like WS_2 nanoparticles: effect of agglomeration, Tribol. Lett. 24 (2006) 225-228.

[16] X. Zhou, H. Shi, X. Fu, D. Wu, Z. Hu, Tribological properties of Cyanex 301 - modified MoS_2 nano - sized hollow spheres in liquid paraffin, Ind. Lubr. Tribol. 60 (2008) 147-152.

[17] P. Rabaso, F. Dassenoy, F. Ville, M. Diaby, B. Vacher, T. Le Mogne, M. Belin, J. Cavoret, An investigation on the reduced ability of IF-MoS_2 nanoparticles to reduce friction and wear in the presence of dispersants, Tribol. Lett. 55 (2014) 503-516.

[18] K.H. Hu, X.G. Hu, Y.F. Xu, F. Huang, J.S. Liu, The Effect of Morphology on the Tribological Properties of MoS_2 in Liquid Paraffin, Tribology Letters 40 (2010) 155-165.

[19] T. Risdon, D. Gresty, An historical review of reductions in fuel consumption of United States and European engines with MoS_2, SAE Technical Paper, 1975.

[20] A. Tomala, B. Vengudusamy, M. Rodríguez Ripoll, A. Naveira Suarez, M. Remškar, R. Rosentsveig, Interaction Between Selected MoS_2 Nanoparticles and ZDDP Tribofilms, Tribology Letters 59 (2015) 1-18.

[21] P.U. Aldana, B. Vacher, T. Le Mogne, M. Belin, B. Thiebaut, F. Dassenoy, Action Mechanism of WS2 Nanoparticles with ZDDP Additive in Boundary Lubrication Regime, Tribology Letters 56 (2014) 249-258.

[22] P. Rabaso, F. Ville, F. Dassenoy, M. Diaby, P. Afanasiev, J. Cavoret, B. Vacher, T. Le Mogne, Boundary lubrication: Influence of the size and structure of inorganic fullerene-like MoS_2 nanoparticles on friction and wear reduction, Wear 320 (2014) 161-178.

[23] L. Joly-Pottuz, J.M. Martin, F. Dassenoy, M. Belin, G. Montagnac, B. Reynard, N. Fleischer, Pressure-induced exfoliation of inorganic fullerene-like WS2 particles in a Hertzian contact, Journal of Applied Physics 99 (2006) 023524.

[24] O. Tevet, P. Von-Huth, R. Popovitz-Biro, R. Rosentsveig, H.D. Wagner, R. Tenne, Friction mechanism of individual multilayered nanoparticles, Proceedings of the National Academy of Sciences of the United States of America 108 (2011) 19901-19906.

[25] X. Zhang, Z. Lai, C. Tan, H. Zhang, Solution-Processed Two-Dimensional MoS_2 Nano-sheets: Preparation, Hybridization, and Applications, Angew Chem Int Ed 55 (2016) 8816-8838.

[26] X. Huang, X. Qi, F. Boey, H. Zhang, Graphene-based composites, Chem. Soc. Rev. 41 (2012) 666-686.

[27] M. Xu, T. Liang, M. Shi, H. Chen, Graphene-like two-dimensional materials, Chem. Rev. 113 (2013) 3766-3798.

[28] O. Lopez-Sanchez, D. Lembke, M. Kayci, A. Radenovic, A. Kis, Ultrasensitive photodetectors based on monolayer MoS_2, Nat. Nanotechnol. 8 (2013) 497-501.

[29] Z. Zeng, Z. Yin, X. Huang, H. Li, Q. He, G. Lu, F. Boey, H. Zhang, Single‐layer semiconducting nano-sheets: High‐yield preparation and device fabrication, Angew Chem Int Ed 50 (2011) 11093-11097.

[30] N. Choudhary, J. Park, J.Y. Hwang, W. Choi, Growth of large-scale and thickness-modulated MoS_2 nano-sheets, Acs Appl. Mater. Interfaces 6 (2014) 21215-21222.

[31] X. Zhang, Z. Lai, C. Tan, H. Zhang, Solution‐processed two‐dimensional MoS_2 nano-sheets: preparation, hybridization, and applications, Angew Chem Int Ed 55 (2016) 8816-8838.

[32] R.J. Smith, P.J. King, M. Lotya, C. Wirtz, U. Khan, S. De, A. O'Neill, G.S. Duesberg, J.C. Grunlan, G. Moriarty, Large‐scale exfoliation of inorganic layered compounds in aqueous surfactant solutions, Adv. Mater. 23 (2011) 3944-3948.

[33] G. Zhang, H. Liu, J. Qu, J. Li, Two-dimensional layered MoS_2: rational design, properties and electrochemical applications, Energy Environ Sci 9 (2016) 1190-1209.

[34] G. Du, Z. Guo, S. Wang, R. Zeng, Z. Chen, H. Liu, Superior stability and high capacity of restacked molybdenum disulfide as anode material for lithium ion batteries, Chem. Commun. 46 (2010) 1106-1108.

[35] G.S. Bang, K.W. Nam, J.Y. Kim, J. Shin, J.W. Choi, S.-Y. Choi, Effective liquid-phase exfoliation and sodium ion battery application of MoS_2 nano-sheets, Acs Appl. Mater. Interfaces 6 (2014) 7084-7089.

[36] S. Wu, Z. Zeng, Q. He, Z. Wang, S.J. Wang, Y. Du, Z. Yin, X. Sun, W. Chen, H. Zhang, Electrochemically reduced single-layer MoS_2 nano-sheets: characterization, properties, and sensing applications, Small 8 (2012) 2264-2270.

[37] H. Li, Z. Yin, Q. He, H. Li, X. Huang, G. Lu, D.W.H. Fam, A.I.Y. Tok, Q. Zhang, H. Zhang, Fabrication of single- and multilayer MoS_2 film-based field-effect transistors for sensing NO at room temperature, Small 8 (2012) 63-67.

[38] Z. Wu, D. Wang, Y. Wang, A. Sun, Preparation and tribological properties of MoS_2 nano-sheets, Adv. Eng. Mater. 12 (2010) 534-538.

[39] H. Huang, J. Tu, L. Gan, C. Li, An investigation on tribological properties of graphite nano-sheets as oil additive, Wear 261 (2006) 140-144.

[40] K.H. Hu, M. Liu, Q.J. Wang, Y.F. Xu, S. Schraube, X.G. Hu, Tribological properties of molybdenum disulfide nano-sheets by monolayer restacking process as additive in liquid paraffin, Tribol. Int. 42 (2009) 33-39.

[41] J. Tannous, F. Dassenoy, I. Lahouij, T. Le Mogne, B. Vacher, A. Bruhács, W. Tremel, Understanding the Tribochemical Mechanisms of IF-MoS_2 Nanoparticles Under Boundary Lubrication, Tribol. Lett. 41 (2011) 55-64.

[42] P.D. Fleischauer, J.R. Lince, A comparison of oxidation and oxygen substitution in MoS_2 solid film lubricants, Tribology International 32 (1999) 627-636.

[43] T. Onodera, Y. Morita, A. Suzuki, M. Koyama, H. Tsuboi, N. Hatakeyama, A. Endou, H. Takaba, M. Kubo, F. Dassenoy, C. Minfray, L. Joly-Pottuz, J.-M. Martin, A. Miyamoto, A Computational Chemistry Study on Friction of h-MoS_2. Part I. Mechanism of Single Sheet Lubrication, The Journal of Physical Chemistry B 113 (2009) 16526-16536.

[44] J. Chen, N. Kuriyama, H. Yuan, H.T. Takeshita, T. Sakai, Electrochemical hydrogen storage in MoS_2 nano-tubes, J. Am. Chem. Soc. 123 (2001) 11813-11814.

[45] M.S. Dresselhaus, G. Dresselhaus, P.C. Eklund, Science of fullerenes and carbon nano-tubes: their properties and applications, Academic press, 1996.

[46] M. Remskar, A. Mrzel, Z. Skraba, A. Jesih, M. Ceh, J. Demšar, P. Stadelmann, F. Lévy, D. Mihailovic, Self-assembly of subnanometer-diameter single-wall MoS_2 nano-tubes, Science 292 (2001) 479-481.

[47] C.M. Zelenski, P.K. Dorhout, Template synthesis of near-monodisperse1 microscale nanofibers and nanotubules of MoS_2, J. Am. Chem. Soc. 120 (1998) 734-742.

[48] M. Nath, A. Govindaraj, C.N.R. Rao, Simple synthesis of MoS_2 and WS_2 nano-tubes, Adv. Mater. 13 (2001) 283-286.

[49] L. Margulis, G. Salitra, R. Tenne, M. Tallanker, Nested fullerene-like structures, Nature 365 (1993) 113-114.

[50] Y. Feldman, E. Wasserman, D. Srolovitz, R. Tenne, High-rate, gas-phase growth of MoS_2 nested inorganic fullerenes and nano-tubes, Science 267 (1995) 222.

[51] F.L. Deepak, M. Jose‐Yacaman, Recent highlights in the synthesis, structure, properties, and applications of MoS_2 nano-tubes, Israel J. Chem. 50 (2010) 426-438.

[52] A. Hassanien, M. Tokumoto, A. Mrzel, D. Mihailovic, H. Kataura, Structural and mechanical properties of MoS_2-I_x nano-tubes and $Mo_6S_xI_y$ nanowires, Physica E 29 (2005) 684-688.

[53] V. Nemanič, M. Žumer, B. Zajec, J. Pahor, M. Remškar, A. Mrzel, P. Panjan, D. Mihailovič, Field-emission properties of molybdenum disulfide nano-tubes, Appl. Phys. Lett. 82 (2003) 4573-4575.

[54] J. Chen, S. Li, Z. Tao, Novel hydrogen storage properties of MoS_2 nano-tubes, J. Alloy. Compd. 356 (2003) 413-417.

[55] J. Chen, S.-L. Li, Q. Xu, K. Tanaka, Synthesis of open-ended MoS_2 nano-tubes and the application as the catalyst of methanation, Chem. Commun. (2002) 1722-1723.

[56] A. Kis, D. Mihailovic, M. Remskar, A. Mrzel, A. Jesih, I. Piwonski, A.J. Kulik, W. Benoît, L. Forró, Shear and Young's moduli of MoS_2 nano-tube ropes, Adv. Mater. 15 (2003) 733-736.

[57] A. Rothschild, S. Cohen, R. Tenne, WS_2 nano-tubes as tips in scanning probe microscopy, Appl. Phys. Lett. 75 (1999) 4025-4027.

[58] R. Tenne, Inorganic nano-tubes and fullerene-like nanoparticles, J. Mater. Res. 21 (2006) 2726-2743.

[59] A.J. Mertens, S. Senthilvelan, Mechanical and tribological properties of carbon nano-tube reinforced polypropylene composites, Proceedings of the Institution of Mechanical Engineers, Part L: Journal of Materials: Design and Applications (2016).

[60] S.-m. Zhou, X.-b. Zhang, Z.-p. Ding, C.-y. Min, G.-l. Xu, W.-m. Zhu, Fabrication and tribological properties of carbon nano-tubes reinforced Al composites prepared by pressureless infiltration technique, Composites Part A: Applied Science and Manufacturing 38 (2007) 301-306.

[61] W. Khalil, A. Mohamed, M. Bayoumi, T.A. Osman, Tribological properties of dispersed carbon nano-tubes in lubricant, Fullerenes, Nano-tubes and Carbon Nanostructures 24 (2016) 479-485.

[62] C.S. Chen, X.H. Chen, L.S. Xu, Z. Yang, W.H. Li, Modification of multi-walled carbon nano-tubes with fatty acid and their tribological properties as lubricant additive, Carbon 43 (2005) 1660-1666.

[63] M. Kalin, J. Kogovšek, M. Remškar, Mechanisms and improvements in the friction and wear behavior using MoS_2 nano-tubes as potential oil additives, Wear 280–281 (2012) 36-45.

[64] K.S. Novoselov, A.K. Geim, S. Morozov, D. Jiang, Y. Zhang, S.a. Dubonos, I. Grigorieva, A. Firsov, Electric field effect in atomically thin carbon films, Science 306 (2004) 666-669.

[65] X. Li, W. Cai, J. An, S. Kim, J. Nah, D. Yang, R. Piner, A. Velamakanni, I. Jung, E. Tutuc, Large-area synthesis of high-quality and uniform graphene films on copper foils, Science 324 (2009) 1312-1314.

[66] F. Bonaccorso, L. Colombo, G. Yu, M. Stoller, V. Tozzini, A.C. Ferrari, R.S. Ruoff, V. Pellegrini, Graphene, related two-dimensional crystals, and hybrid systems for energy conversion and storage, Science 347 (2015) 1246501.

[67] R. Raccichini, A. Varzi, S. Passerini, B. Scrosati, The role of graphene for electrochemical energy storage, Nature Mater. 14 (2015) 271-279.

[68] K.-H. Wu, H.-H. Cheng, A.A. Mohammad, I. Blakey, K. Jack, I.R. Gentle, D.-W. Wang, Electron-beam writing of deoxygenated micro-patterns on graphene oxide film, Carbon 95 (2015) 738-745.

[69] J. Yao, X. Shi, W. Zhai, A.M.M. Ibrahim, Z. Xu, L. Chen, Q. Zhu, Y. Xiao, Q. Zhang, Z. Wang, The enhanced tribological properties of NiAl intermetallics: combined lubrication of multilayer graphene and WS_2, Tribol. Lett. 56 (2014) 573-582.

[70] K.S. Novoselov, A.K. Geim, S.V. Morozov, D. Jiang, Y. Zhang, S.V. Dubonos, I.V. Grigorieva, A.A. Firsov, Electric field effect in atomically thin carbon films, Science 306 (2004) 666-669.

[71] Y. Hernandez, V. Nicolosi, M. Lotya, F.M. Blighe, Z. Sun, S. De, I. McGovern, B. Holland, M. Byrne, Y.K. Gun'Ko, High-yield production of graphene by liquid-phase exfoliation of graphite, Nat. Nanotechnol. 3 (2008) 563-568.

[72] Y. Xu, J. Geng, X. Zheng, K.D. Dearn, X. Hu, Friction-induced transformation from graphite dispersed in esterified bio-oil to graphene, Tribol. Lett. 63 (2016) 1-11.

[73] C. Oshima, A. Nagashima, Ultra-thin epitaxial films of graphite and hexagonal boron nitride on solid surfaces, J Phys: Condens Matter 9 (1997) 1-20.

[74] W. Yang, G. Chen, Z. Shi, C.-C. Liu, L. Zhang, G. Xie, M. Cheng, D. Wang, R. Yang, D. Shi, K. Watanabe, T. Taniguchi, Y. Yao, Y. Zhang, G. Zhang, Epitaxial growth of single-domain graphene on hexagonal boron nitride, Nat Mater 12 (2013) 792-797.

[75] M. Fumihiko, H. Hiroki, Molecular beam epitaxial growth of graphene and ridge-structure networks of graphene, J Phys D: Appl Phys 44 (2011) 435305.

[76] A. Reina, X. Jia, J. Ho, D. Nezich, H. Son, V. Bulovic, M.S. Dresselhaus, J. Kong, Large area, few-layer graphene films on arbitrary substrates by chemical vapor deposition, Nano Lett. 9 (2008) 30-35.

[77] X. Li, C.W. Magnuson, A. Venugopal, R.M. Tromp, J.B. Hannon, E.M. Vogel, L. Colombo, R.S. Ruoff, Large-area graphene single crystals grown by low-pressure chemical vapor deposition of methane on copper, J. Am. Chem. Soc. 133 (2011) 2816-2819.

[78] S.V. Tkachev, E.Y. Buslaeva, A.V. Naumkin, S.L. Kotova, I.V. Laure, S.P. Gubin, Reduced graphene oxide, Inorg. Mater. 48 (2012) 796-802.

[79] A.K. Geim, A.H. Macdonald, Graphene: exploring carbon flatland, Phys. Today 60 (2007) 35.

[80] T.-T. Shan, S. Xin, Y. You, H.-P. Cong, S.-H. Yu, A. Manthiram, Combining nitrogen-doped graphene sheets and MoS_2: a unique film–foam–film structure for enhanced lithium storage, Angewandte Chemie (2016) n/a-n/a.

[81] I.W. Frank, D.M. Tanenbaum, A.M. van der Zande, P.L. McEuen, Mechanical properties of suspended graphene sheets, J. Vac. Sci. Technol. B 25 (2007) 2558-2561.

[82] G. Van Lier, C. Van Alsenoy, V. Van Doren, P. Geerlings, Ab initio study of the elastic properties of single-walled carbon nano-tubes and graphene, Chem. Phys. Lett. 326 (2000) 181-185.

[83] Y. Zhu, S. Murali, W. Cai, X. Li, J.W. Suk, J.R. Potts, R.S. Ruoff, Graphene and graphene oxide: Synthesis, properties, and applications, Adv. Mater. 22 (2010) 3906-3924.

[84] C. Lee, X. Wei, J.W. Kysar, J. Hone, Measurement of the elastic properties and intrinsic strength of monolayer graphene, Science 321 (2008) 385-388.

[85] L.A. Falkovsky, Optical properties of graphene, J Phys Conf Ser 129 (2008) 012004.

[86] J. Lin, L. Wang, G. Chen, Modification of Graphene Platelets and their Tribological Properties as a Lubricant Additive, Tribology Letters 41 (2010) 209-215.

[87] V. Eswaraiah, V. Sankaranarayanan, S. Ramaprabhu, Graphene-based engine oil nanofluids for tribological applications, ACS Appl Mater Interfaces 3 (2011) 4221-4227.

[88] W. Zhang, M. Zhou, H. Zhu, Y. Tian, K. Wang, J. Wei, F. Ji, X. Li, Z. Li, P. Zhang, D. Wu, Tribological properties of oleic acid-modified graphene as lubricant oil additives, Journal of Physics D: Applied Physics 44 (2011) 205303.

[89] M. Kalin, J. Kogovšek, M. Remškar, Mechanisms and improvements in the friction and wear behavior using MoS_2 nano-tubes as potential oil additives, Wear 280–281 (2012) 36-45.

[90] C. Wang, H. Li, Y. Zhang, Q. Sun, Y. Jia, Effect of strain on atomic-scale friction in layered MoS_2, Tribol. Int. 77 (2014) 211-217.

[91] P. Rabaso, F. Ville, F. Dassenoy, M. Diaby, P. Afanasiev, J. Cavoret, B. Vacher, T. Le Mogne, Boundary lubrication: Influence of the size and structure of inorganic fullerene-like MoS_2 nanoparticles on friction and wear reduction, Wear 320 (2014) 161-178.

[92] M. Marquart, M. Wahl, S. Emrich, G. Zhang, B. Sauer, M. Kopnarski, B. Wetzel, Enhancing the lifetime of MoS_2-lubricated ball bearings, Wear 303 (2013) 169-177.

[93] J. Kogovšek, M. Remškar, A. Mrzel, M. Kalin, Influence of surface roughness and running-in on the lubrication of steel surfaces with oil containing MoS_2 nano-tubes in all lubrication regimes, Tribol. Int. 61 (2013) 40-47.

[94] W. Zhang, D. Demydov, M.P. Jahan, K. Mistry, A. Erdemir, A.P. Malshe, Fundamental understanding of the tribological and thermal behavior of Ag–MoS_2 nanoparticle-based multi-component lubricating system, Wear 288 (2012) 9-16.

[95] Z.Y. Xu, Y. Xu, K.H. Hu, Y.F. Xu, X.G. Hu, Formation and tribological properties of hollow sphere-like nano-MoS_2 precipitated in TiO_2 particles, Tribol. Int. 81 (2015) 139-148.

[96] L.-Y. Lin, D.-E. Kim, W.-K. Kim, S.-C. Jun, Friction and wear characteristics of multi-layer graphene films investigated by atomic force microscopy, Surf Coat Technol 205 (2011) 4864-4869.

[97] S.S. Kandanur, M.A. Rafiee, F. Yavari, M. Schrameyer, Z.-Z. Yu, T.A. Blanchet, N. Koratkar, Suppression of wear in graphene polymer composites, Carbon 50 (2012) 3178-3183.

[98] D. Berman, A. Erdemir, A.V. Sumant, Few layer graphene to reduce wear and friction on sliding steel surfaces, Carbon 54 (2013) 454-459.

[99] L. Zhang, J. Pu, L. Wang, Q. Xue, Frictional dependence of graphene and carbon nano-tube in diamond-like carbon/ionic liquids hybrid films in vacuum, Carbon 80 (2014) 734-745.

[100] X. Fan, L. Wang, Highly Conductive Ionic Liquids toward High-Performance Space-Lubricating Greases, Acs Appl. Mater. Interfaces 6 (2014) 14660-14671.

[101] Z. Huang, W. Han, X. Liu, X. Qi, J. Zhong, Graphene/MoS_2 hybrid structure and its photoresponse property, Ceram. Int. 40 (2014) 11971-11974.

[102] Q. Feng, K. Duan, X. Ye, D. Lu, Y. Du, C. Wang, A novel way for detection of eugenol via poly (diallyldimethylammonium chloride) functionalized graphene-MoS_2 nano-flower fabricated electrochemical sensor, Sens Actuators, B 192 (2014) 1-8.

[103] C. Zhai, M. Zhu, D. Bin, F. Ren, C. Wang, P. Yang, Y. Du, Two dimensional MoS_2/graphene composites as promising supports for Pt electrocatalysts towards methanol oxidation, J. Power Sources 275 (2015) 483-488.

[104] L. Ma, J. Ye, W. Chen, D. Chen, J. Yang Lee, Gemini surfactant assisted hydrothermal synthesis of nanotile-like MoS_2/graphene hybrid with enhanced lithium storage performance, Nano Energy 10 (2014) 144-152.

[105] Y. Xu, Y. Peng, K.D. Dearn, X. Zheng, L. Yao, X. Hu, Synergistic lubricating behaviors of graphene and MoS_2 dispersed in esterified bio-oil for steel/steel contact, Wear 342 (2015) 297-309.

[106] Y.F. Xu, X.J. Zheng, Y.G. Yin, J. Huang, X.G. Hu, Comparison and analysis of the influence of test conditions on the tribological properties of emulsified bio-oil, Tribol. Lett. 55 (2014) 543-552.

[107] Y. Xu, X. Zheng, X. Hu, K.D. Dearn, H. Xu, Effect of catalytic esterification on the friction and wear performance of bio-oil, Wear 311 (2014) 93-100.

[108] M. JF, W. Stickle, S. PE, B. KD, Handbook of X-ray photoelectron spectroscopy, Phys. Electronics Inc, Eden Prairie, 1995.